Solving PDE's with FEniCS

Laplace and Poisson

Chapters 1–7

Introduction to

Automated Modeling

with FEniCS

by L. Ridgway Scott

Partial differential equations (PDEs) are used to model everything.

Finite element method (FEM) solves general PDEs in complex geometry.

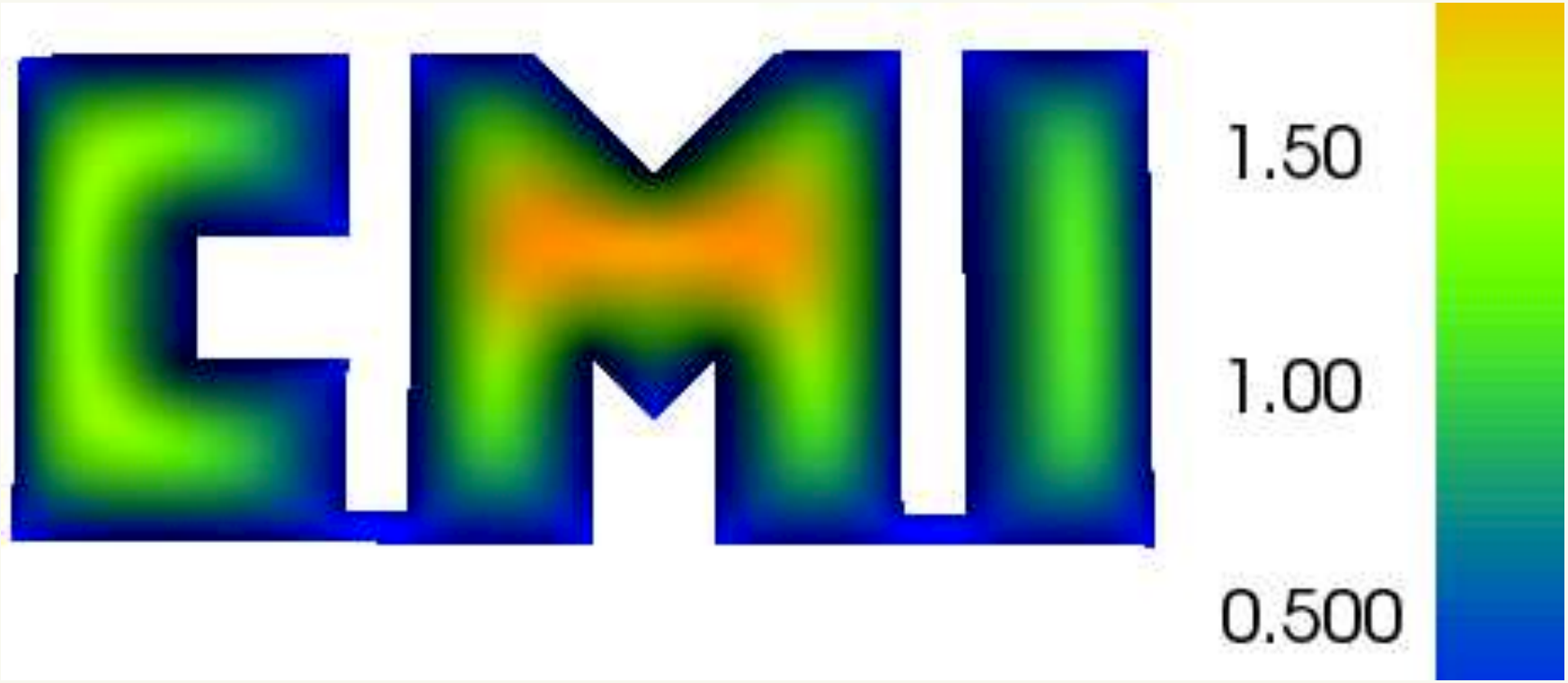

Variational formulations

Finite element method based on variational formulation of partial differential equations (PDEs).

The variational formulation provides three things:

- Language to define PDEs for compilation into executable code
- Foundation for theory of PDEs that allows one to know whether or not a given model is well posed
- Framework (Galerkin) for numerical approximation

We explain first two via a simple example, Laplace's equation.

Subsequently, a large variety of problems will be shown to fit into this framework.

PDEs are difficult

PDEs are difficult. They faithfully represent reality.

Singularities occur when you least expect them.

FEM ideally suited to simulate such behavior.

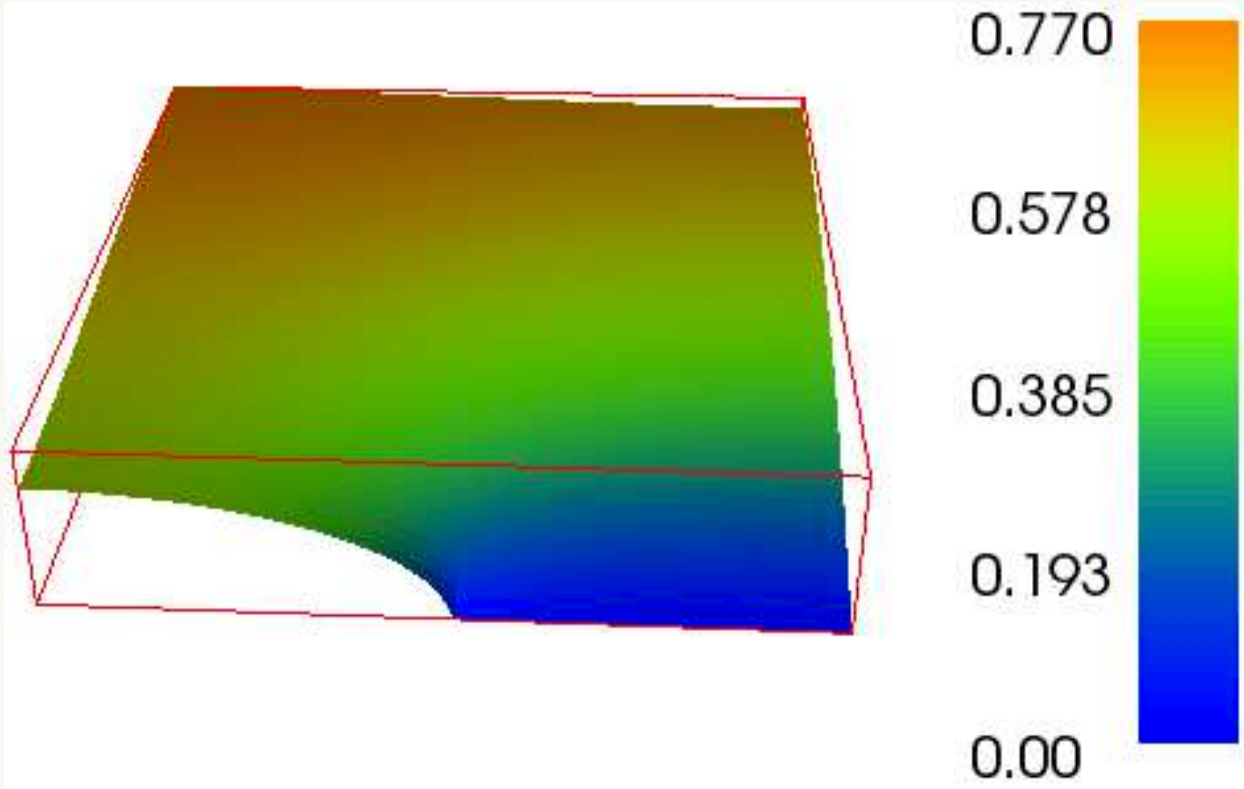

Laplace equation

Define a function u in a domain $\Omega \subset \mathbb{R}^d$ by

$$-\Delta u = f \text{ in } \Omega \tag{1}$$

together with boundary conditions

$$\begin{aligned} u &= 0 \text{ on } \Gamma \subset \partial\Omega \qquad \text{(Dirichlet)} \\ \frac{\partial u}{\partial n} &= 0 \text{ on } \partial\Omega \backslash \Gamma \qquad \text{(Neumann)} \end{aligned} \tag{2}$$

where $\frac{\partial u}{\partial n}$ denotes the derivative of u in the direction normal to the boundary, $\partial\Omega$ ($\frac{\partial u}{\partial n} = \mathbf{n} \cdot \nabla u$.)

This is known variously as Poisson's equation or Laplace's equation (especially when $f \equiv 0$).

Laplace applications

This equation forms the basis of a remarkable number of physical models.

It serves as a basic equation for diffusion, elasticity, electrostatics, gravitation, and many more domains.

In potential flow, the gradient of u is the velocity of incompressible, inviscid, irrotational fluid flow.

- The boundary $\partial\Omega$ is the surface of an obstacle moving in the flow, and one solves the equation on the exterior of Ω.

The right box for solutions

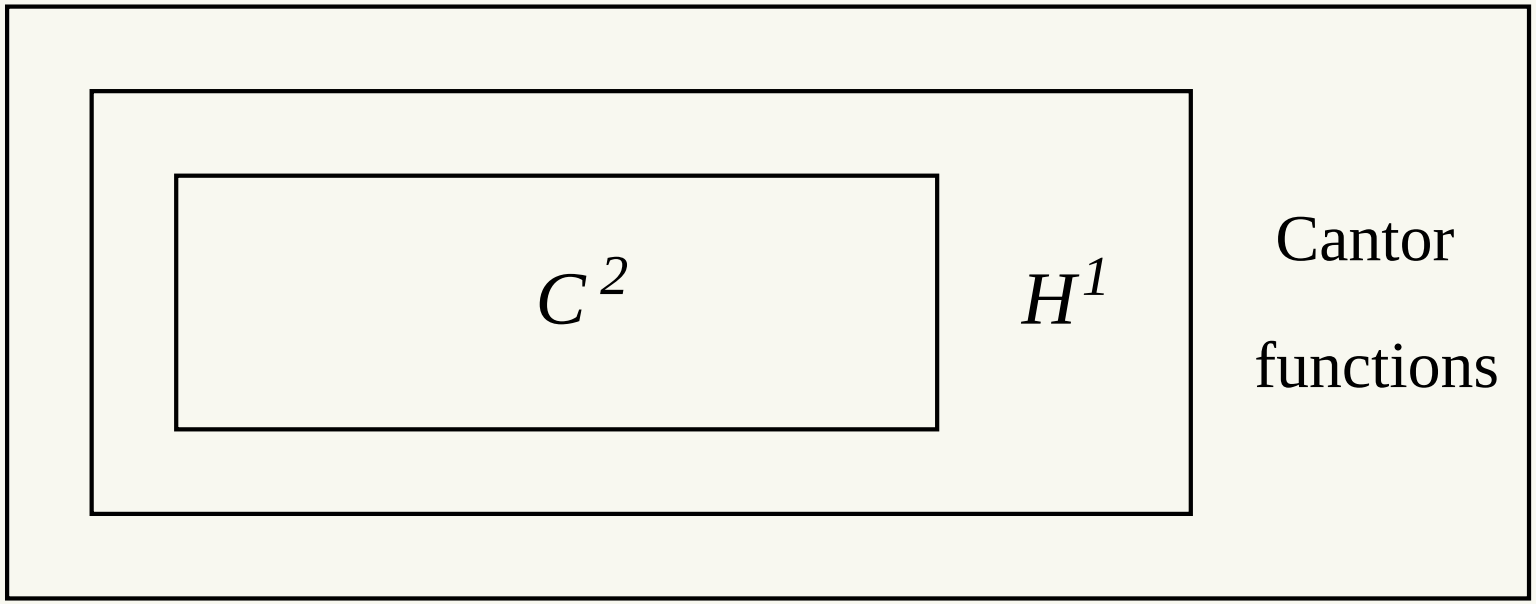

Different possible spaces in which to look for a solution.

- One is too big, so that spurious solutions abound, as described in Section 27.3.
- One is too small, so that many physically relevant solutions do not exist in that space,
- But Sobolev spaces are just right.

Solution space

Right place to look for solution of such an equation is a Sobolev space denoted $H^1(\Omega)$ defined by

$$H^1(\Omega) = \left\{ v \in L^2(\Omega) \ : \ \nabla v \in L^2(\Omega)^d \right\},$$

where $L^2(\Omega)$ means functions square integrable on Ω:

$$\|v\|_{L^2(\Omega)} = \left(\int_\Omega v(\mathbf{x})^2 \, d\mathbf{x} \right)^{1/2} < \infty,$$

$L^2(\Omega)^d$ means d copies of $L^2(\Omega)$ (Cartesian product).

There is a natural inner-product on $L^2(\Omega)$ defined by

$$(v, w)_{L^2(\Omega)} = \int_\Omega v(\mathbf{x}) \, w(\mathbf{x}) \, d\mathbf{x},$$

Inner-product and associated norm on $H^1(\Omega)$ defined by

$$(v, w)_{H^1(\Omega)} = (v, w)_{L^2(\Omega)} + \int_\Omega \nabla v(\mathbf{x}) \cdot \nabla w(\mathbf{x})\, d\mathbf{x}$$

$$\|v\|_{H^1(\Omega)} = \sqrt{(v, v)_{H^1(\Omega)}}$$

For a vector-valued function $\mathbf{w}$, e.g., $\mathbf{w} = \nabla v$, we define

$$\|\mathbf{w}\|_{L^2(\Omega)} = \| \, |\mathbf{w}| \, \|_{L^2(\Omega)} = \Big(\int_\Omega |\mathbf{w}(\mathbf{x})|^2 \, d\mathbf{x} \Big)^{1/2},$$

where $|\xi|$ denotes Euclidean norm of vector $\xi \in \mathbb{R}^d$, and

$$(\mathbf{v}, \mathbf{w})_{L^2(\Omega)} = \int_\Omega \mathbf{v}(\mathbf{x}) \cdot \mathbf{w}(\mathbf{x})\, d\mathbf{x}.$$

Domain for Poisson's Equation

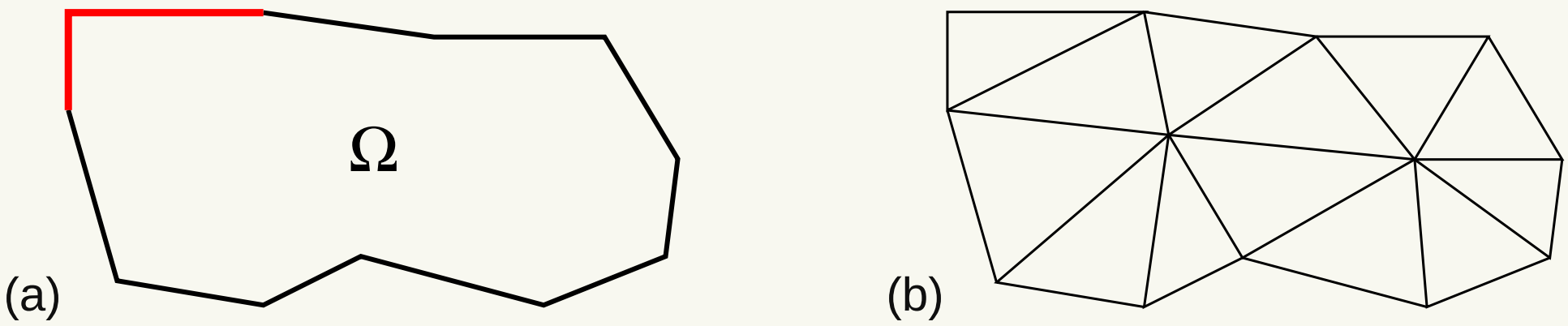

Figure 3: (a) Domain Ω with Γ indicated in red. (b) Triangulation of Ω.

Now consider equation (1) with boundary conditions (2).

Assume Γ has nonzero measure (length or area, or even volume, depending on dimension).

Later, we will return to the case when Γ is empty, the pure Neumann case.

Typical Ω shown in Figure 3, with Γ shown in red.

Boundary condtions for Poisson's Equation

To formulate the variational equivalent of (1) with boundary conditions (2), we define a variational space that incorporates the essential, i.e., Dirichlet, part of the boundary conditions in (2):

$$V := \left\{ v \in H^1(\Omega) \ : \ v|_\Gamma = 0 \right\}. \tag{3}$$

See Table 1 for an explanation of the various names used to describe different boundary conditions.

generic name	example	honorific name
essential	$u = 0$	Dirichlet
natural	$\frac{\partial u}{\partial n} = 0$	Neumann

Table 1: Nomenclature for different types of boundary conditions.

Variational Formulation of Poisson's Equation

Bilinear form for variational problem determined by

(1) multiplying equation by a nice function v,

(2) integrating over Ω and then

(3) integrating by parts:

$$
\begin{aligned}
(f, v)_{L^2(\Omega)} &= \int_\Omega (-\Delta u) v \, d\mathbf{x} \\
&= \int_\Omega \nabla u \cdot \nabla v \, d\mathbf{x} - \oint_{\partial\Omega} v \frac{\partial u}{\partial n} \, ds \qquad (4) \\
&= \int_\Omega \nabla u \cdot \nabla v \, d\mathbf{x} := a(u, v).
\end{aligned}
$$

The boundary term in (4) vanishes for $v \in V$ because either v or $\frac{\partial u}{\partial n}$ is zero on any part of the boundary.

The integration-by-parts formula derives from the divergence theorem

$$\int_\Omega \nabla\cdot \mathbf{w}(\mathbf{x})\, d\mathbf{x} = \oint_{\partial\Omega} \mathbf{w}(s)\cdot\mathbf{n}(s)\, ds$$

applied to $\mathbf{w} = v\nabla u$, together with $\frac{\partial u}{\partial n} = (\nabla u)\cdot\mathbf{n}$ and $\Delta u = \nabla\cdot(\nabla u)$ ($\mathbf{n}$ is the outward-directed normal to $\partial\Omega$). More precisely, we observe that

$$\begin{aligned}\nabla\cdot(v\nabla u) &= \sum_{i=1}^{d} \left((v\nabla u)_i\right)_{,i} = \sum_{i=1}^{d} (v\, u_{,i})_{,i} \\ &= \sum_{i=1}^{d} v_{,i}u_{,i} + v\, u_{,ii} = \nabla v\cdot\nabla u + v\Delta u.\end{aligned}$$

Thus the divergence theorem applied to $\mathbf{w} = v\nabla u$ gives

$$\oint_{\partial\Omega} v\nabla u(s)\cdot\mathbf{n}(s)\,ds = \int_{\Omega}\big(\nabla\cdot(v\nabla u)\big)(\mathbf{x})\,d\mathbf{x}$$
$$= \int_{\Omega}(\nabla v\cdot\nabla u + v\Delta u)(\mathbf{x})\,d\mathbf{x},$$

which means that

$$\int_{\Omega} -v(\mathbf{x})\Delta u(\mathbf{x})\,d\mathbf{x} = \int_{\Omega}\nabla v(\mathbf{x})\cdot\nabla u(\mathbf{x})\,d\mathbf{x} - \oint_{\partial\Omega} v\,\frac{\partial u}{\partial n}\,ds \qquad (5)$$
$$= a(u,v) - \oint_{\partial\Omega} v\,\frac{\partial u}{\partial n}\,ds.$$

Thus, u can be characterized via

$$u \in V \text{ satisfies}$$
$$a(u,v) = (f,v)_{L^2(\Omega)} \quad \forall v \in V. \tag{6}$$

The reverse result, namely

a solution to the variational problem in (6) solves Poisson's equation

can be proved for smooth u.

Sketched later and done in detail in the one-dimensional case.

Variational formulation translates to the following code:

```
from dolfin import *
# Create mesh and define function space
mesh = UnitSquareMesh(32, 32)
V = FunctionSpace(mesh, "Lagrange", 1)
# Define boundary condition
u0 = Constant(0.0)
bc = DirichletBC(V, u0, "on_boundary")
# Define variational problem
u = TrialFunction(V)
v = TestFunction(V)
pi=3.141592
you = Expression("(sin(pi*x[0]))*(sin(pi*x[1]))",degree=1)
a = inner(grad(u), grad(v))*dx
L = (2*pi*pi)*you*v*dx
# Compute solution
u = Function(V)
solve(a == L, u, bc)
plot(u, interactive=True)
```

Plot of the solution

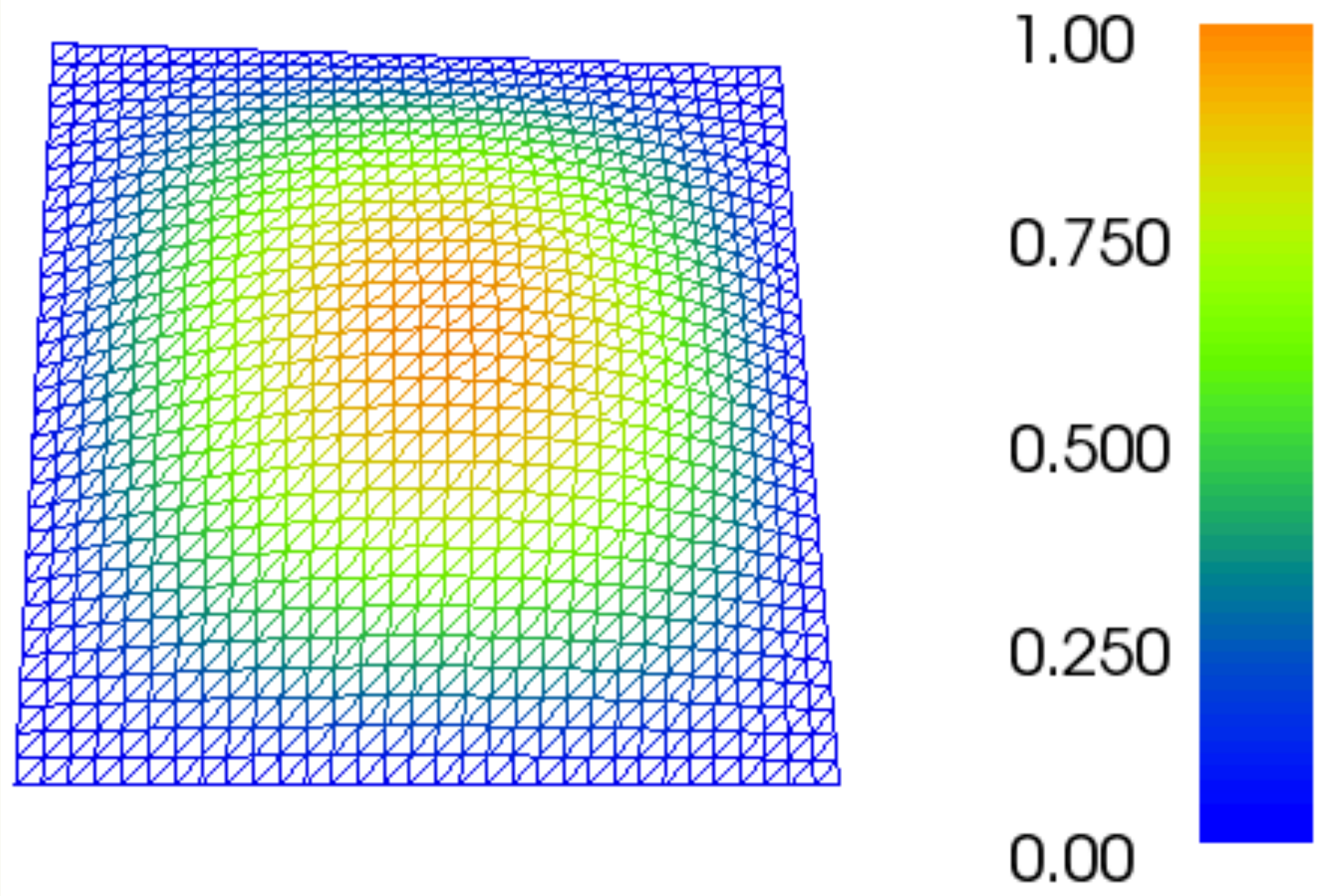

The variational forms

```
from dolfin import *
# Create mesh and define function space
mesh = UnitSquareMesh(32, 32)
V = FunctionSpace(mesh, "Lagrange", 1)
# Define boundary condition
u0 = Constant(0.0)
bc = DirichletBC(V, u0, "on_boundary")
# Define variational problem
u = TrialFunction(V)
v = TestFunction(V)
pi=3.141592
you = Expression("(sin(pi*x[0]))*(sin(pi*x[1])",degre
a = inner(grad(u), grad(v))*dx
L = (2*pi*pi)*you*v*dx
# Compute solution
u = Function(V)
solve(a == L, u, bc)
plot(u, interactive=True)
```

Forms can include user-defined Expressions.

The domain and function space

```
from dolfin import *
# Create mesh and define function space
mesh = UnitSquareMesh(32, 32)
V = FunctionSpace(mesh, "Lagrange", 1)
# Define boundary condition
u0 = Constant(0.0)
bc = DirichletBC(V, u0, "on_boundary")
# Define variational problem
u = TrialFunction(V)
v = TestFunction(V)
pi=3.141592
you = Expression("(sin(pi*x[0]))*(sin(pi*x[1]))",degree=1)
a = inner(grad(u), grad(v))*dx
L = (2*pi*pi)*you*v*dx
# Compute solution
u = Function(V)
solve(a == L, u, bc)
plot(u, interactive=True)
```

The domain is the union of elements in the mesh.

The boundary conditions

```
from dolfin import *
# Create mesh and define function space
mesh = UnitSquareMesh(32, 32)
V = FunctionSpace(mesh, "Lagrange", 1)
# Define boundary condition
u0 = Constant(0.0)
bc = DirichletBC(V, u0, "on_boundary")
# Define variational problem
u = TrialFunction(V)
v = TestFunction(V)
pi=3.141592
you = Expression("(sin(pi*x[0]))*(sin(pi*x[1]))",degree=1)
a = inner(grad(u), grad(v))*dx
L = (2*pi*pi)*you*v*dx
# Compute solution
u = Function(V)
solve(a == L, u, bc)
plot(u, interactive=True)
```

Constant is a special Expression.

Solving the equations and plotting

```
from dolfin import *
# Create mesh and define function space
mesh = UnitSquareMesh(32, 32)
V = FunctionSpace(mesh, "Lagrange", 1)
# Define boundary condition
u0 = Constant(0.0)
bc = DirichletBC(V, u0, "on_boundary")
# Define variational problem
u = TrialFunction(V)
v = TestFunction(V)
pi=3.141592
you = Expression("(sin(pi*x[0]))*(sin(pi*x[1]))",degree=1)
a = inner(grad(u), grad(v))*dx
L = (2*pi*pi)*you*v*dx
# Compute solution
u = Function(V)
solve(a == L, u, bc)
plot(u, interactive=True)
```

Different versions may plot differently.

Meaning of `dolfin` code

The code `f*dx` means

$$\int_\Omega f(x)\,dx$$

where Ω is the domain associated with the function space of which f is a member:

$$f \in V, \quad \Omega = \text{domain}(V)$$

In our example, V is defined by

```
V = FunctionSpace(mesh, "Lagrange", 1)
```

and `mesh` contains the domain information.

A manufactured solution

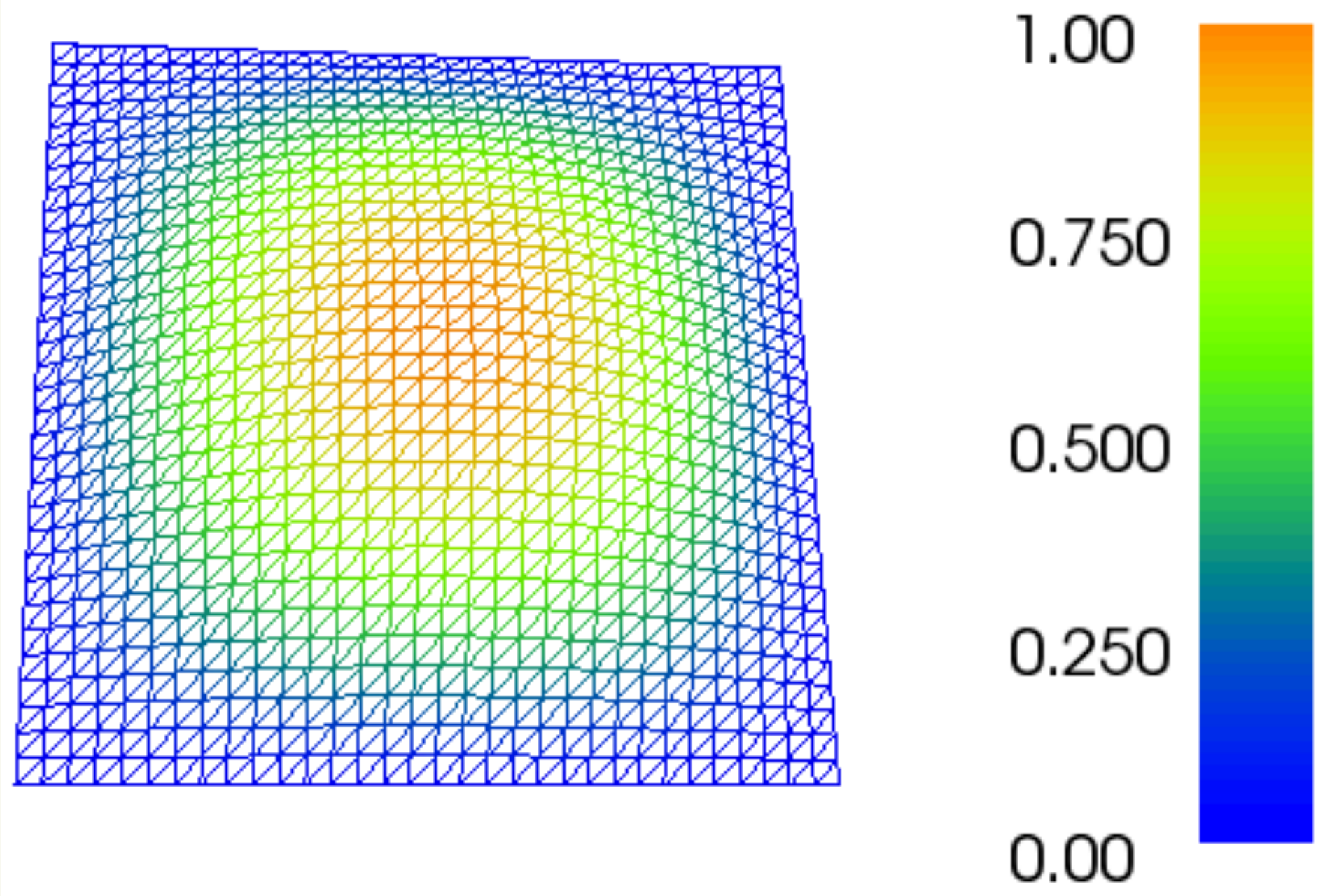

Method of manufactured solutions

Method of manufactured solutions tests our technology by considering a problem with a known solution:

$$-\Delta u = 2\pi^2 \sin(\pi x)\sin(\pi y) \text{ in } \Omega = [0,1]\times[0,1]$$
$$u = 0 \text{ on } \partial\Omega,$$

whose solution is $u(x,y) = \sin(\pi x)\sin(\pi y)$.

Of course, we started with the solution

$$u(x,y) = \sin(\pi x)\sin(\pi y)$$

and then computed its Laplacian to get

$$f = 2\pi^2 \sin(\pi x)\sin(\pi y).$$

Dirichlet boundary condition specification

In line 9, the third variable in `DirichletBC` specifies where Dirichlet boundary conditions are to be specified.

Table 2 specifies two other ways of achieving same thing, for example

```
bc=DirichletBC(V,u0,DomainBoundary())
```

technique	specification
keyword	`"on_boundary"`
reserved function	`DomainBoundary()`
user defined function	`boundary`

Table 2: Different ways to specify the boundary of a domain.

Variational formulations as theory

We have seen that

- variational formulations provide a language

for partial differential equations (PDEs).

Now we show that

- variational formulations provide a basis

for the theory of PDEs.

This gives us greater confidence in the validity of our technical simulations.

Linear functionals as data

A function F defined on V is called a linear functional if

it is a linear function defined for any $v \in V$

having a real number as its value.

The right-hand side of (6) can be written using

$$F(v) = (f, v)_{L^2(\Omega)} \quad \forall v \in V. \tag{7}$$

The expression F is called a linear functional because (a) it is linear and (b) it has scalar values.

By linear, we mean that

$$F(u + av) = F(u) + aF(v)$$

for any scalar a and any $u, v \in V$.

Continuous linear functionals

Critical condition on a linear functional for success in a variational formulation: *bounded* (a.k.a. *continuous*).

A linear functional F is bounded (equivalently continuous) on a normed space V if

$$|F(v)| \leq C_F \|v\|_V \quad \forall v \in V. \tag{8}$$

A natural norm $\|\cdot\|_V$ for the space V defined in (3) is

$$\|v\|_a = \sqrt{a(v,v)}.$$

The smallest possible constant C_F for which

(8) holds is called the dual norm of F.

Dual norm

The **dual norm** of F is defined by

$$\|F\|_{V'} := \sup_{0 \neq v \in V} \frac{|F(v)|}{\|v\|_V}. \tag{9}$$

The linear form (7)

$$F(v) = (f, v)_{L^2(\Omega)} \quad \forall v \in V$$

is bounded on $H^1(\Omega)$: L^2 norm is part of H^1 norm.

But other linear forms are not, such as $F(v) := v'(x_0)$ for some $x_0 \in [0, 1]$.

This form is linear, but consider what it should do for the function $v(x) := |x - x_0|^{2/3}$. Note that $v \in H^1([0, 1])$.

Inhomogeneous Neumann problem

Illustrates need for linear functionals as data.

Consider Laplace equation (1) with inhomogeneous Neumann boundary condition

$$\frac{\partial u}{\partial n} = g \text{ on } \Omega \backslash \Gamma.$$

As before, we assume homogeneous Dirichlet boundary conditions posed on $\Gamma \subset \partial\Omega$, and we define

$$V = \left\{ v \in H^1(\Omega) \ : \ v = 0 \text{ on } \Gamma \right\}.$$

From (5) we get variational form: $u \in V$ with

$$a(u, v) = (f, v)_{L^2(\Omega)} + \oint_{\partial\Omega \backslash \Gamma} g(s) v(s) \, ds \qquad \forall v \in V.$$

Inhomogeneous Neumann linear form

Yet another example of the general variational problem

$$u \in V \text{ satisfying } a(u,v) = F(v) \quad \forall v \in V, \tag{10}$$

where the linear functional F is given by

$$F(v) = (f,v)_{L^2(\Omega)} + \oint_{\partial\Omega\setminus\Gamma} g(s)v(s)\,ds \quad \forall v \in V.$$

Can prove F is continuous on $H^1(\Omega)$.

Shows why we need general concept of linear forms as data.

Inhomogeneous Neumann example

Consider $\Omega = [0,1]^2$ with homogeneous Dirichlet data on

$$\Gamma = \{(x,y) \in \partial\Omega \ : \ x = 0 \text{ or } y = 0 \text{ or } y = 1\}.$$

Thus $\Omega \backslash \Gamma = \{(x,y) \in \partial\Omega \ : \ x = 1\}$. The variational formulation of

$$-\Delta u = f \text{ in } \Omega, \quad u = 0 \text{ on } \Gamma, \quad \frac{\partial u}{\partial n} = g \text{ on } \partial\Omega \backslash \Gamma \qquad (11)$$

is to find $u \in V = \left\{v \in H^1(\Omega) \ : \ v = 0 \text{ on } \Gamma\right\}$ such that

$$a(u,v) = (f,v)_{L^2(\Omega)} + \oint_{\partial\Omega\backslash\Gamma} g(s)v(s)\,ds \quad \forall v \in V, \qquad (12)$$

where as before $a(u,v) = \int_\Omega \nabla u(\mathbf{x}) \cdot \nabla v(\mathbf{x})\,d\mathbf{x}$.

Inhomogeneous Neumann example

Define $g(y) = y(1-y)$ and $f(x,y) = 2x$.

As always, define $V = \left\{ v \in H^1(\Omega) \ : \ v = 0 \text{ on } \Gamma \right\}$.

Exact solution is $u(x,y) = xy(1-y)$.

The solution is depicted in Figure 4.

degree	mesh size	L^2 error
1	32	1.78e-04
2	8	3.87e-05
3	2	1.51e-15

Table 3: Errors for inhomogeneous Neumann problem.

Inhomogeneous Neumann example

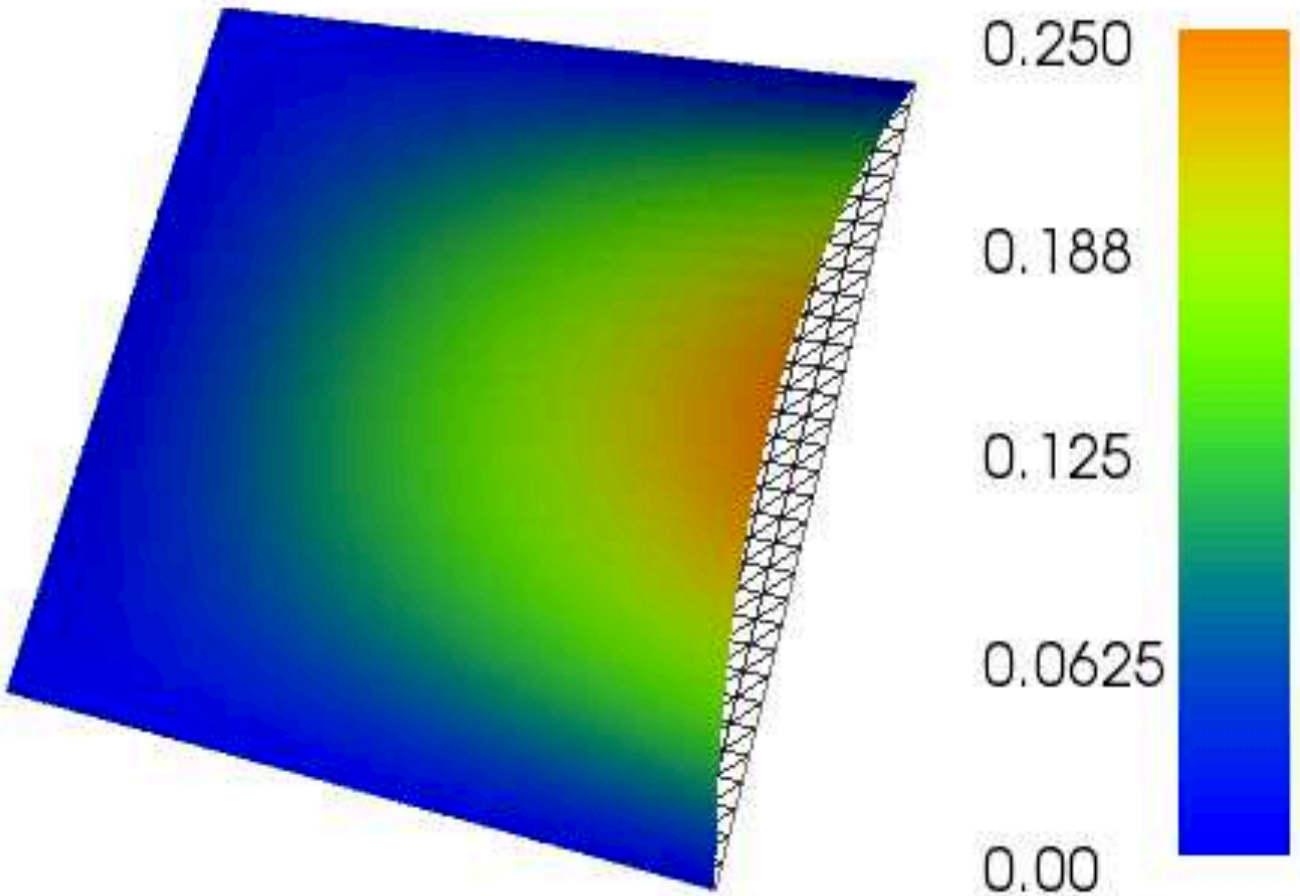

Figure 4: Solution of (11) computed using piecewise linears on a 32×32 mesh.

Varying variational formulations

We have seen that Laplace's equation can be expressed as a variational formulation

Find $u \in V$ such that

$$a(u, v) = F(v) \text{ for all } v \in V$$

and furthermore that the variational formulation can be used as a language to describe the problem in code.

Now we want to show that this formulation is universal for a broad range of problems.

Formulation of the Pure Neumann Problem: varying V

Pure Neumann (or natural) boundary conditions

$$\frac{\partial u}{\partial n} = 0 \text{ on } \partial\Omega \tag{13}$$

(i.e., when $\Gamma = \emptyset$) varies the definition of V.

In particular, solutions are unique only up to an additive constant, and they can exist only if the right-hand side f in (1) satisfies

$$\begin{aligned}\int_\Omega f(\mathbf{x})\,d\mathbf{x} &= \int_\Omega -\Delta u(\mathbf{x})\,d\mathbf{x} \\ &= \int_\Omega \nabla u(\mathbf{x}) \cdot \nabla 1\,d\mathbf{x} - \oint_{\partial\Omega} \frac{\partial u}{\partial n}\,ds = 0.\end{aligned}$$

Mean-zero spaces

A variational space appropriate for the present case is

$$V = \left\{ v \in H^1(\Omega) \ : \ \int_\Omega v(\mathbf{x})\, d\mathbf{x} = 0 \right\}. \tag{14}$$

For any integrable function g, we define its *mean*, $\bar{g}$, as follows:

$$\bar{g} := \frac{1}{\text{meas}(\Omega)} \int_\Omega g(\mathbf{x})\, d\mathbf{x}.$$

For any $v \in H^1(\Omega)$, note that $v - \bar{v} \in V$.

Then $u - \bar{u}$ satisfies the variational formulation (6) with V defined as in (14).

Conversely, if $u \in H^2(\Omega)$ solves the variational equation (6) with V defined as in (14), then u solves Poisson's equation (1) with a right-hand-side given by

$$\tilde{f}(\mathbf{x}) := f(\mathbf{x}) - \bar{f} \quad \forall \mathbf{x} \in \Omega \tag{15}$$

with boundary conditions (13).

Why does this work?

Variational form $a(\cdot, \cdot)$ is *coercive* on V [2]: there is a constant C depending only on Ω such that

$$\|v\|^2_{H^1(\Omega)} \leq C a(v, v) \quad \forall v \in V.$$

Coercivity requires removal of constants from V.

Dirichlet data on small part Γ of boundary does this: if a constant is zero on Γ it is zero everywhere.

Poincaré's inequality says that

$$\|v - \overline{v}\|^2_{L^2(\Omega)} \leq Ca(v,v) \quad \forall v \in H^1(\Omega).$$

For $v \in V$, the mean $\overline{v}$ is zero. Thus

$$\|v\|^2_{L^2(\Omega)} \leq Ca(v,v) \quad \forall v \in V.$$

Squaring and adding $a(v,v)$ to both sides gives

$$\|v\|^2_{H^1(\Omega)} = a(v,v) + \|v\|^2_{L^2(\Omega)} \leq (C^2+1)a(v,v) \quad \forall v \in V.$$

Proving continuity

Easy to see that reverse holds:

$$a(v,v) \leq C\|v\|^2_{H^1(\Omega)}$$

for all $v \in V$.

This *continuity* condition and the Cauchy-Schwarz inequality (20) guarantee $a(u,v)$ makes sense for $u, v \in V$.

The coercivity and continuity bounds hold for discrete approximations as well under a very simple condition:

$$V_h \subset V.$$

Bilinear forms

An expression $a(\cdot, \cdot)$ is **bilinear form** if it is linear in each argument separately. Fix $w \in V$ and define forms

$$F(v) = a(v, w) \quad \text{and} \quad G(v) = a(w, v) \quad \text{for all } v \in V.$$

We require that F and G be linear. More concretely,

$$a(u + cv, w) = a(u, w) + ca(v, w) \text{ and}$$

$$a(u, cv + w) = ca(u, v) + a(u, w)$$

for all $u, v, w \in V$ and any constant c.

Variational form $a(u, v) = \int_\Omega \nabla u \cdot \nabla v \, d\mathbf{x}$ is bilinear because integral of sum of functions is sum of integrals.

Critical foundation of PDE theory is coercivity condition:

$$\|v\|^2_{H^1(\Omega)} \leq Ca(v,v) \quad \forall v \in V. \tag{16}$$

Coercivity implies solution is unique: $f \equiv 0 \implies$

$$0 = (f,u)_{L^2} = a(u,u) \geq \frac{1}{C}\|u\|^2_{H^1(\Omega)}.$$

Coercivity condition implies a stability result:

$$\|u\|_{H^1(\Omega)} \leq \frac{Ca(u,u)}{\|u\|_{H^1(\Omega)}} = C\frac{(f,u)_{L^2}}{\|u\|_{H^1(\Omega)}} \leq C\|f\|_{V'}, \tag{17}$$

where dual norm defined by

$$\|F\|_{V'} := \sup_{0 \neq v \in V} \frac{|F(v)|}{\|v\|_V}.$$

Continuity condition

Finite-dimensional case: uniqueness implies existence.

Infinite dimensions, **continuity condition** required:

$$|a(u,v)| \le C\|u\|_{H^1(\Omega)}\|v\|_{H^1(\Omega)} \quad \text{for all } u,v \in V. \qquad (18)$$

Usually this condition is evident, but consider

$$-\frac{1}{2}\Delta u(r_1,r_2) + \left(\kappa(r_1)+\kappa(r_2)\right)u(r_1,r_2) = f(r_1,r_2)$$

in $\Omega = [0,\infty]\times[0,\infty]$, where $\kappa(r) = r^{-2} - r^{-1} + \frac{1}{2}$.

Here coercivity is easy but continuity requires Hardy's inequality (assuming $u = 0$ on $\partial\Omega$).

Lax-Milgram Theorem Suppose $a(\cdot,\cdot)$ is coercive (16) and continuous (18) (bounded) on $H^1(\Omega)$.

Then variational problem (6) has unique solution u for every continuous (bounded) F defined on $H^1(\Omega)$, and

$$\|u\|_{H^1(\Omega)} \leq c_1 c_0 \sup_{v \in H^1(\Omega)} \frac{|F(v)|}{\|v\|_{H^1(\Omega)}},$$

where c_0 is constant in (16) and c_1 is constant in (18).

The combination of continuity and coercivity correspond to the **stability** of the numerical scheme.

A small detail

Our definition of the variational space V ensures that $a(v, v) < \infty$ for all $v \in V$.

But our variational formulation involves $a(u, v)$ for $u, v \in V$.

Why is $a(u, v)$ well defined for all $u, v \in V$?

The Cauchy-Schwarz inequality guarantees that

$$|a(u, v)| \leq \|u\|_a \|v\|_a,$$

where $\|v\|_a = \sqrt{a(v, v)}$ for all $v \in V$.

The proof is a simple calculation.

Cauchy-Schwarz inequality proof

$$\begin{aligned} a(u - tv, u - tv) &= a(u, u) - 2ta(v, u) + t^2 a(v, v) \\ &= a(u, u) - 2ta(u, v) + t^2 a(v, v). \end{aligned}$$

In particular, since $a(u - tv, u - tv) \geq 0$,

$$2ta(u, v) \leq a(u, u) + t^2 a(v, v). \tag{19}$$

For example, suppose that $a(v, v) = 0$.

Choose the sign of t to be the sign of $a(u, v)$. From (19) we conclude that

$$2|t|\,|a(u, v)| \leq a(u, u).$$

Since $2|t|\,|a(u, v)| \leq a(u, u)$ holds for all $t \in \mathbb{R}$, we can let $|t| \to \infty$ to conclude that $a(u, v) = 0$.

Cauchy-Schwarz inequality

If $a(v,v) \neq 0$, define $t = \text{sign}(a(u,v))\|u\|_a/\|v\|_a$.

If by chance $a(u,u) = 0$, then we reverse the previous argument to conclude that again $a(u,v) = 0$.

If not zero, and thus $t \neq 0$, divide by $|t|$ in (19) to get

$$2|a(u,v)| \leq \frac{1}{|t|}a(u,u) + |t|\, a(v,v) = 2\|u\|_a\|v\|_a.$$

Thus we have proved the Cauchy-Schwarz inequality

$$|a(u,v)| \leq \|u\|_a\|v\|_a. \tag{20}$$

The Cauchy-Schwarz inequality is generally true for any non-negative, symmetric bilinear form.

Inner products

Cauchy-Schwarz often stated for an **inner-product**.

Our bilinear form $a(\cdot, \cdot)$ is almost an inner-product except that it lacks one condition, non-degeneracy.

In our case $a(v, v) = 0$ if v is constant, and for an inner-product, this is not allowed.

One example of an inner-product is the bilinear form

$$(u, v)_{L^2(\Omega)} = \int_\Omega u(x)\, v(x)\, dx.$$

Here we see that $(v, v)_{L^2(\Omega)} = 0$ implies that $v \equiv 0$.

But the Cauchy-Schwarz inequality does not require this additional property to be valid.

Connection to classical notions

Suppose that $u \in C^2(\Omega)$ and V is defined by (3). Recall the integration-by-parts formula (4), which we write as

$$\int_\Omega (-\Delta u) v \, d\mathbf{x} = a(u, v) + \oint_{\partial\Omega} v \frac{\partial u}{\partial n} \, ds. \tag{21}$$

If $a(u, v) = (f, v)_{L^2(\Omega)}$ for all $v \in V$, then

$$\int_\Omega \big((-\Delta u)(\mathbf{x}) - f(\mathbf{x})\big) v(\mathbf{x}) \, d\mathbf{x} = \oint_{\partial\Omega} v(s) \frac{\partial u}{\partial n}(s) \, ds.$$

We can choose $v \in V$ to be zero on the boundary, and in this case

$$\int_\Omega \big((-\Delta u)(\mathbf{x}) - f(\mathbf{x})\big) v(\mathbf{x}) \, d\mathbf{x} = 0.$$

Implications of smoothness

In particular, suppose that f and Δu are continuous and

$$(-\Delta u)(\mathbf{x}_0) - f(\mathbf{x}_0) \neq 0$$

for some $\mathbf{x}_0 \in \Omega$ satisfying

$$d := \text{distance}(\mathbf{x}_0, \partial\Omega) > 0.$$

Then there is an $\epsilon > 0$ such that $\epsilon < d$ and

$$|(-\Delta u)(\mathbf{x}) - f(\mathbf{x})| > 0 \text{ for all } |\mathbf{x} - \mathbf{x}_0| < \epsilon.$$

Choose

$$v(\mathbf{x}) = \begin{cases} 1 - \epsilon^{-1}|\mathbf{x} - \mathbf{x}_0| & |\mathbf{x} - \mathbf{x}_0| < \epsilon \\ 0 & |\mathbf{x} - \mathbf{x}_0| \geq \epsilon \end{cases}. \tag{22}$$

Variatonal equation

Note that $v \geq 0$ and $v > 0$ for $|\mathbf{x} - \mathbf{x}_0| < \epsilon$, and that $v \in H_0^1(\Omega)$ (exersize).

But this would mean that

$$\int_\Omega \big((-\Delta u)(\mathbf{x}) - f(\mathbf{x})\big) v(\mathbf{x})\, d\mathbf{x} \neq 0,$$

yielding a contradiction.

This means that wherever both f and Δu are continuous, we must have $f = -\Delta u$.

So that the variational solution is also a classical solution if it is smooth enough.

Meaning of naturual boundary conditions

From previous arguments, $-\Delta u = f$ in Ω provided both continuous on Ω.

Thus integration-by-parts formula (21) implies

$$\int_\Omega f(\mathbf{x})v(\mathbf{x})\,d\mathbf{x} = a(u,v) + \oint_{\partial\Omega} v(s)\,\frac{\partial u}{\partial n}(s)\,ds$$

for all $v \in V$.

Comparing (21) and (10), we conclude that

$$\oint_{\partial\Omega} g(s)v(s)\,ds = \oint_{\partial\Omega} v(s)\,\frac{\partial u}{\partial n}(s)\,ds = \oint_{\partial\Omega\setminus\Gamma} v(s)\,\frac{\partial u}{\partial n}(s)\,ds$$

for all $v \in V$, where V is defined by (3).

More meaning of naturual boundary conditions

Suppose that $s_0 \in \partial\Omega \backslash \Gamma$ with distance$(s_0, \Gamma) > 0$, and suppose that $g(s_0) - \frac{\partial u}{\partial n}(s_0) \neq 0$.

If both g and $\frac{\partial u}{\partial n}$ are continuous near s_0, there is an $\epsilon > 0$ such that $|g(s) - \frac{\partial u}{\partial n}(s)| > 0$ for all $s \in \partial\Omega$ satisfying $|s - s_0| < \epsilon$.

Choose v as in (22). Then we reach a contradiction:

$$\oint_{\partial\Omega\backslash\Gamma} v(s)\left(g(x) - \frac{\partial u}{\partial n}(s)\right) ds \neq 0.$$

Thus we conclude that $\frac{\partial u}{\partial n}(s) = g(s)$ wherever they are both continuous (as well as Δu and f).

Variational formulation: find $u \in V$ such that

$$a(u, v) = F(v) \text{ for all } v \in V$$

gives PDE language and theory.

Also provides basis for numerical methods.

The key idea, due to Galerkin, is to construct a set of functions $V_h \subset V$ and then to

find $u_h \in V_h$ such that

$$a(u_h, v) = F(v) \text{ for all } v \in V_h$$

Domain subdivisions

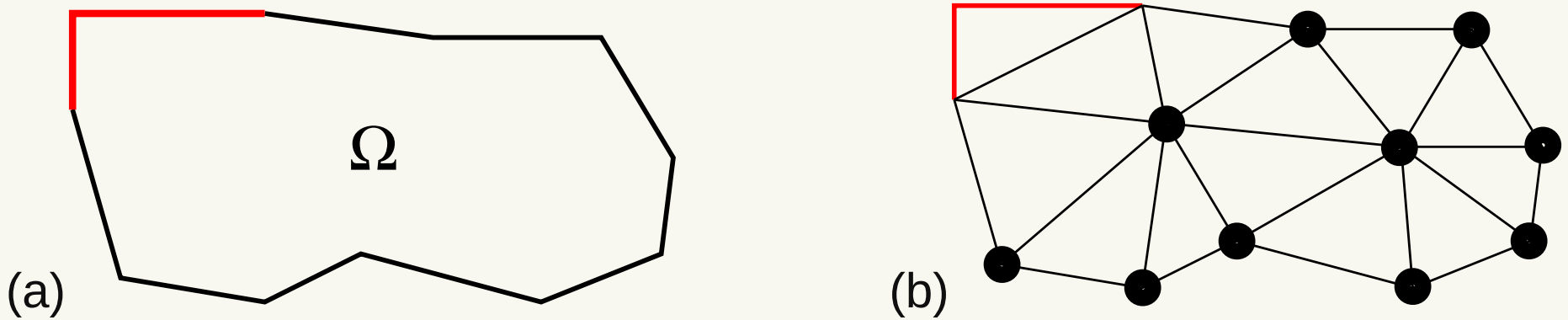

Let T_h denote a subdivision of Ω, e.g., a triangulation (triangles in two-D or tetrahedra in three-D).

Triangulation of the domain in (a) is shown in (b).

The main requirement for a triangulation is that no vertex of a triangle can be in the middle of an edge.

However, more general subdivisions can be used that violate this property [1, 8, 9].

Using elements

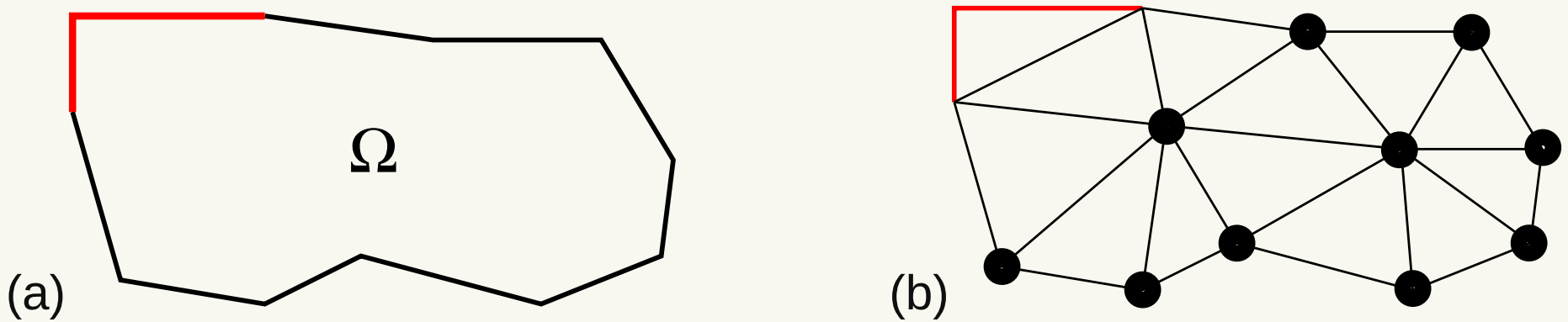

Figure 5: (a) Domain Ω with Γ indicated in red. (b) Nodal positions for V_h are indicated by the black dots; note that vertices in Γ are not included, to respect the essential (Dirichlet) boundary condition.

Main concept of finite element method: use each element of the subdivision as a separate domain in which to reason about the balance of forces.

Mathematically, corresponds to choosing functions on each element to represent variables used in the model.

Using the coercivity condition

Often, same functions used on each element, but not necessary [8, 9, 5].

In this way, one constructs a finite dimensional space V_h which can be used in what is known as the **Galerkin method** to approximate the variational formulation (6), as follows:

$$\text{find } u_h \in V_h \text{ satisfying } a(u_h, v) = (f, v) \quad \forall v \in V_h. \quad (23)$$

Here we can think of h as designating the subdivision,

or perhaps as a parameter that denotes the size of the elements of the subdivision.

Using the coercivity condition

The coercivity condition implies stability for the discrete approximation, namely

$$\|u_h\|_{H^1(\Omega)} \leq \frac{Ca(u_h, u_h)}{\|u_h\|_{H^1(\Omega)}} = C\frac{(f, u_h)}{\|u_h\|_{H^1(\Omega)}} \leq C\|f\|_{V'}, \quad (24)$$

where we will explain the meaning of $\|f\|_{V'}$ later.

In particular, if $f \equiv 0$, then $u_h \equiv 0$.

Provided V_h is finite dimensional, this implies that (23) always has a unique solution.

We can see this more clearly by choosing a basis $\{\phi_i \in V_h \ : \ i = 1, \ldots, N_h\}$. Write $u_h = \sum_i U_i \phi_i$.

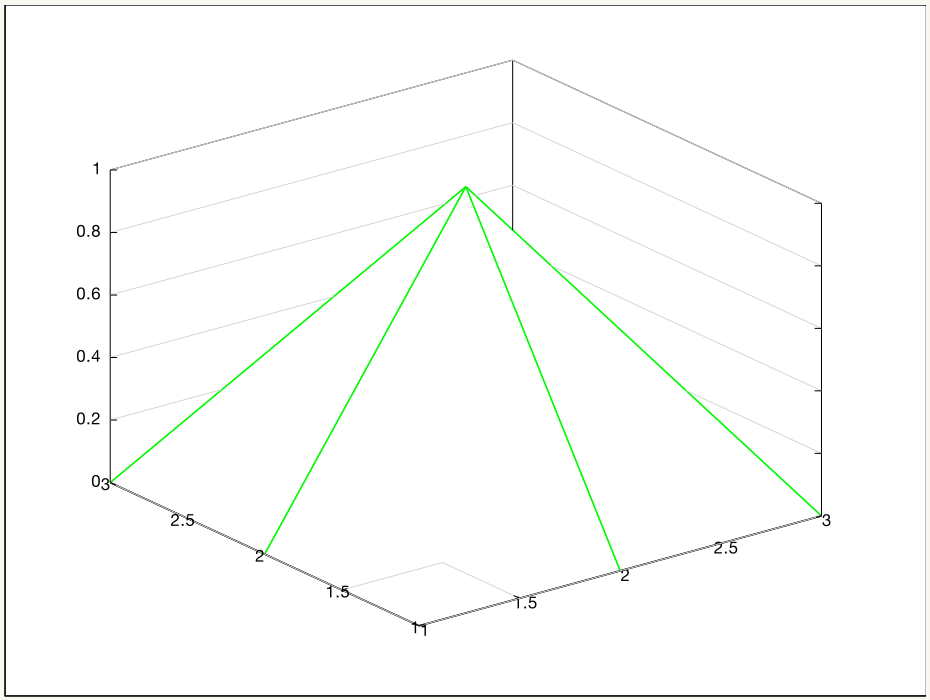

Figure 6: Typical basis function for continuous piecewise linear functions.

Using the linearity of the form $a(\cdot,\cdot)$ in each of its variables, we obtain the linear system $AU = F$ where

$$A_{ij} = a(\phi_i, \phi_j), \;\; F_i = \int_\Omega f(\mathbf{x})\, \phi_i(\mathbf{x})\, d\mathbf{x} \;\forall i, j = 1, \ldots, N_h.$$

Since A is symmetric ($A_{ji} = a(\phi_j, \phi_i) = a(\phi_i, \phi_j) = A_{ij}$), we have, for all $j = 1, \ldots, N_h$,

$$F_j = \int_\Omega f(\mathbf{x})\, \phi_j(\mathbf{x})\, d\mathbf{x} = a(u_h, \phi_j) = a\Big(\sum_i U_i \phi_i, \phi_j\Big)$$
$$= \sum_i U_i a(\phi_i, \phi_j) = \sum_i U_i A_{ij} = \sum_i A_{ji} U_i = \big(AU\big)_j$$

From linear algebra, solution to linear system $AU = F$ exists uniquely $\iff$ only solution for $F = \mathbf{0}$ is $U = \mathbf{0}$.

The latter is guaranteed by the coercivity condition (17):

$$\|u_h\|^2_{H^1(\Omega)} \leq C a(u_h, u_h) = C(f, u_h) = 0.$$

Piecewise linears

Given a triangulation, the simplest space V_h that we can construct is the set of continuous piecewise linear functions.

On each triangle (or tetrahedron), such functions are linear, and moreover we contrive to make them continuous.

A linear function is determined by its values at the vertices of a simplex.

Easy to see in one or two dimensions; graph of function is line or plane through specified values at vertices.

If values of $v \in V_h$ at vertices agree in all of the triangles meeting there, then resulting function is continuous.

Kronecker basis

In two dimensions, the values along edges are specified completely by the values at the vertices.

A basis for V_h satisfies $\phi_i(\mathbf{x}_j) = \delta_{ij}$ (Kronecker δ) as depicted in Figure 6.

The vertices of a triangulation provide the **nodes** of the space V_h; these are shown as black dots in Figure 5.

Only vertices where nodal values are non-zero have black dots, where the boundary condition $v = 0$ holds on Γ for $v \in V_h \subset V$.

General approximation

What determines the accuracy of the approximation?

Céa's Theorem [2, 2.8.1] says the following.

Suppose that $V_h \subset V$, that the variational form $a(\cdot, \cdot)$ is bounded and coercive on V, and that F is bounded on V. Then

$$\|u - u_h\|_a \leq C \inf_{v \in V_h} \|u - v\|_a.$$

Thus the accuracy of the finite element method is determined by the accuracy of approximation.

Often called quasi-optimal.

Nodal values for quadratics

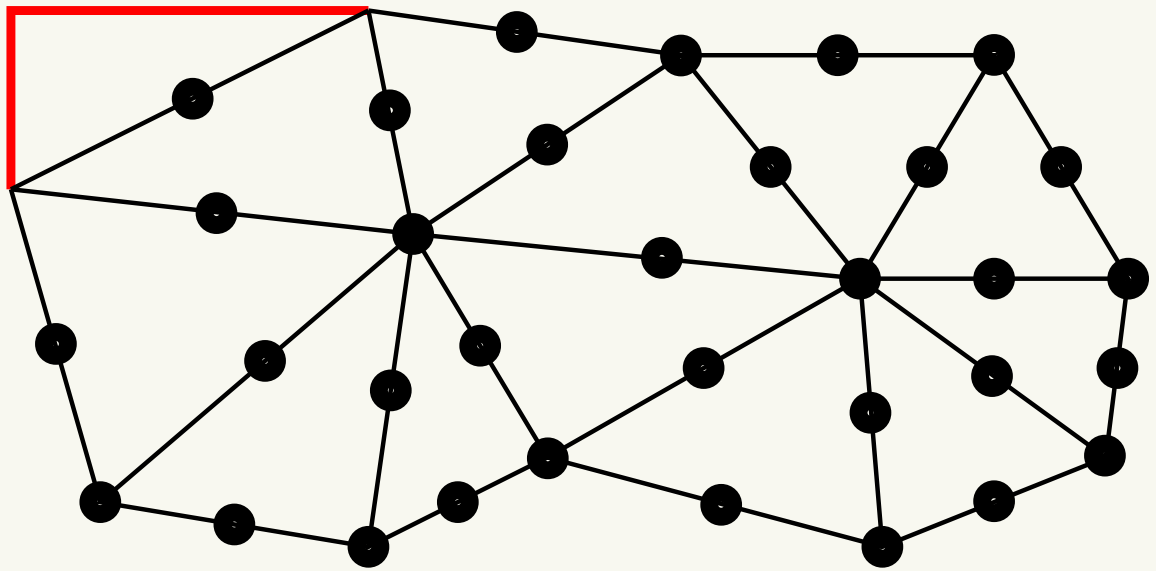

Figure 7: Nodes for quadratics: vertices and edge midpoints.

For more accurate, cost effective approximation, often useful to use higher-order polynomials in each element.

In Figure 7 we see the nodes for piecewise quadratic functions (compare Figure 3).

Piecewise quadratic approximation

Again, we can define a basis for the space V_h of continuous piecewise quadratics in terms of functions that satisfy

$$\phi_i(\mathbf{x}_j) = \delta_{ij} \text{ (Kronecker } \delta\text{)},$$

where the $\mathbf{x}_j$'s are the nodes in Figure 7.

But now it is not so clear how we can be sure that this is a valid representation.

What we need to know is that this nodal representation is **unisolvent** on each triangle, meaning that

> on each triangle you can solve uniquely for a quadratic given the values at the specified nodes, the vertices and edge midpoints.

Proof of unisolvence: degree reduction

On each edge, we have three distinct points that determine uniquely a quadratic, simply by invoking the fundamental theorem of algebra.

If all nodal values on one edge vanish, then the quadratic $q(x, y)$ must vanish on that edge.

WLOG suppose that edge lies on the x-axis. Then $q(x, y) = y\ell(x, y)$ where ℓ is a linear polynomial in x, y.

Can be verified by expanding q in powers of x and y (there are 6 terms) and invoking $q(x, y) \equiv 0$ on the edge lying on the x-axis.

Proof of unisolvence continued

q also vanishes on the other two edges of the triangle, neither of which can lie on the x-axis, so that means that ℓ must also vanish on these edges.

But this clearly implies that $\ell \equiv 0$, and thus $q \equiv 0$.

By linear algebra, uniqueness of the representation implies existence of a representation:

> We have exactly 6 nodal variables matching the dimension of space of quadratic polynomials in two dimensions.

Complete details are found in [2, Chapter 3].

Arbitrary degree polynomials

No limit on the degree of polynomials that can be used.

General family of elements called **Lagrange elements**.

Regular pattern of nodes shown in Figure 8.

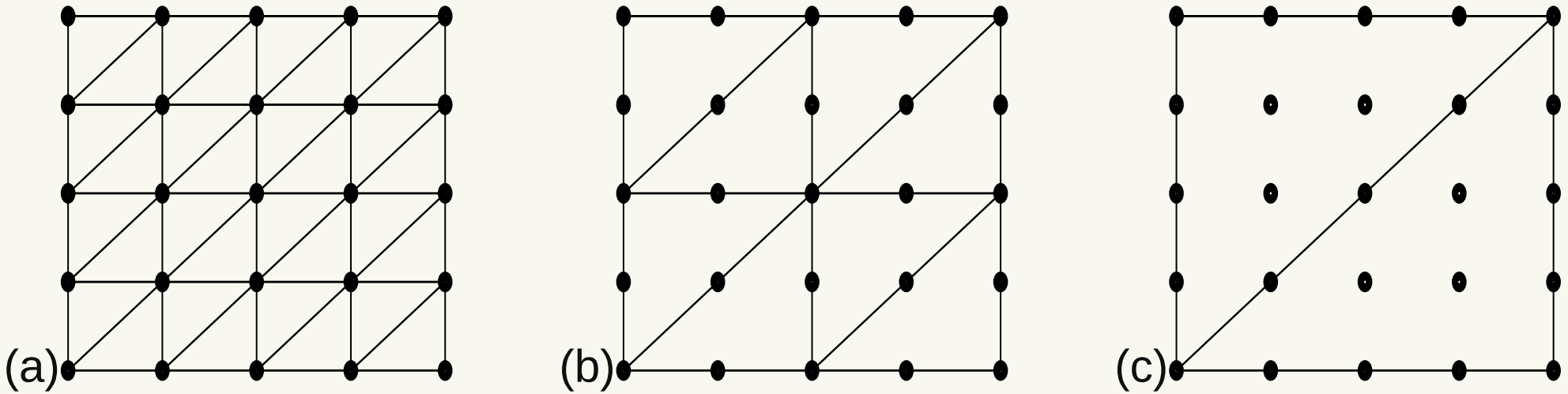

Figure 8: Varying mesh number M and polynomial degree k with the same number of nodes: (a) $M = 4$, $k = 1$ (linears), (b) $M = 2$, $k = 2$ (quadratics), (c) $M = 1$, $k = 4$ (quartics).

Using the method of manufactured solutions, consider

$$\begin{aligned} -\Delta u &= 2\pi^2 \sin(\pi x)\sin(\pi y) \text{ in } \Omega = [0,1]\times[0,1] \\ u &= 0 \text{ on } \partial\Omega, \end{aligned} \tag{25}$$

whose solution is $u(x,y) = \sin(\pi x)\sin(\pi y)$.

The errors

$$\|u_h - u\|_{L^2(\Omega)} = \|u_h - (2\pi^2)^{-1} f\|_{L^2(\Omega)} \tag{26}$$

for different meshes shown in Figure 8 and different polynomial degrees, together with execution times, are given in Table 4.

Computational experiments with (25).

degree	mesh number	L^2 error	time (s)
1	32	2.11e-03	0.09
2	8	5.65e-04	0.08
1	128	1.32e-04	0.31
2	16	6.93e-05	0.08
1	256	3.31e-05	1.07
2	64	1.08e-06	0.23
4	8	7.78e-07	0.08
8	2	7.29e-08	0.08
4	16	2.44e-08	0.11
16	1	1.61e-09	0.09
4	32	7.64e-10	0.23
8	4	1.42e-10	0.09
4	64	2.39e-11	0.74
4	128	4.95e-12	3.0
8	8	3.98e-12	0.13
8	16	1.67e-11	0.33

Table 4: Computational experiments with solving the problem (25).

Arbitrary degree polynomials

What we see in Table 4 is that the error can be reduced substantially by using higher-order polynomials.

Increasing the mesh number for linear Lagrange elements does reduce the error, but the execution time grows commensurately with the error reduction.

Using linears on a mesh of size 256 gives half the error of quadratics on a mesh of size 16, but the latter computation requires one-tenth of the time.

For the same amount of time as this computation with quadratics, using quartics on a mesh of size 8 gives an error almost two orders of magnitude smaller.

Arbitrary degree polynomials

Each mesh with double the number of mesh points was derived from the one with the smaller number of points by subdiving each triangle into four similar triangles.

To get the highest accuracy, the best strategy is to use higher polynomial order, up to a point.

The most accurate computation occurs with polynomial degree 8 with a mesh number of 8.

But the error quits decreasing at a certain point due to round-off error.

Will discuss the effects of finite precision arithmetic is more detail later.

Arbitrary degree polynomials

The times presented here should be viewed as approximate.

There is significant variation due to system load from run to run.

These computations were done on a MacBook Pro with 2.3 GHz Intel Core i7 and 16 GB 1600 MHz DDR3 memory.

However, we do see order of magnitude variation depending on the mesh size and polynomial degree.

Now we review the theory behind

convergence of finite element method.

Céa's Theorem says:

just depends on approximation theory.

Degree of polynomials determines
best rate of approximation.

Success in the finite element method is guaranteed by

- continuous and coercive bilinear form $a(\cdot, \cdot)$
- bounded (continuous) linear form F (data)
- good approximation by V_h (Céa's Theorem)

Just need to understand

why piecewise polynomials

provide good approximation.

Nodal basis means good approximation

Nodal basis key to finite element error behavior.

Both piecewise linears and piecewise quadratics have

nodal basis functions ϕ_i which satisfy $\phi_i(x_j) = \delta_{ij}$ (Kronecker δ), where x_j denotes a typical node.

For linears, the nodes are the vertices, and

for quadratics the edge midpoints are added.

For higher degree Lagrange elements, more edge nodes are involved, as well as interior nodes.

With cubics, the centroid of each triangle is a node.

Interpolant

Nodal representation is basis for defining an interpolant.

Using such a nodal representation, we construct a

global interpolant I_h

defined on continuous functions, by

$$I_h u = \sum_i u(\mathbf{x}_i)\phi_i.$$

Thus I_h maps continuous functions into the space V_h used in finite element computations.

Interpolant approximation

Let I_h denote a global interpolant for a family of finite elements based on the components of $\mathcal{T}^h$.

Suppose that $I_h u$ is continuous, as is true for the Lagrange family of elements.

Further, suppose that the corresponding shape functions have an approximation order, m, that is

$$\|u - I_h u\|_{H^1(\Omega)} \leq C h^{m-1} |u|_{H^m(\Omega)}. \tag{27}$$

In order to have good approximation, we need to have

$$I_h \left(V \cap C^k(\Omega) \right) \subset V_h, \tag{28}$$

where $k = 0$ for Lagrange elements.

However, we allow for the possibility that $k > 0$ since this holds for other element families.

Condition $I_h\left(V \cap C^k(\Omega)\right) \subset V_h$, is a mesh constraint.

If $V_h \subset V$ and the form $a(\cdot, \cdot)$ is bounded and coercive, then unique solution, $u_h \in V_h$, to variational problem

$$a(u_h, v) = (f, v) \quad \forall v \in V_h$$

satisfies (by Céa's theorem)

$$\begin{aligned}\|u - u_h\|_{H^1(\Omega)} &\leq C \inf_{v \in V_h} \|u - v\|_{H^1(\Omega)} \\ &\leq C\|u - I_h u\|_{H^1(\Omega)} \leq Ch^{m-1}|u|_{H^m(\Omega)}.\end{aligned}$$

Summary: if conditions (27) and (28) hold, then

$$\|u - u_h\|_{H^1(\Omega)} \leq Ch^{m-1}|u|_{H^m(\Omega)}.$$

The requirements $V_h \subset V$ and (28) place a constraint on the subdivision in the case that Γ is neither empty nor all of the boundary.

These requirements provide the **consistency** of the numerical approximation.

Necessary to choose the mesh so that it aligns properly with the points where the boundary conditions change from Dirichlet to Neumann.

Matching Boundary Conditions

If the points where the boundary conditions change are vertices in the triangulation, then

$$V_h := I_h \left(V \cap C^0(\Omega) \right)$$

is same as space of piecewise polynomials that vanish on edges contained in Γ.

If we choose mesh so that edges contained in Γ form a subdivision of Γ, it follows that $V_h \subset V$ holds.

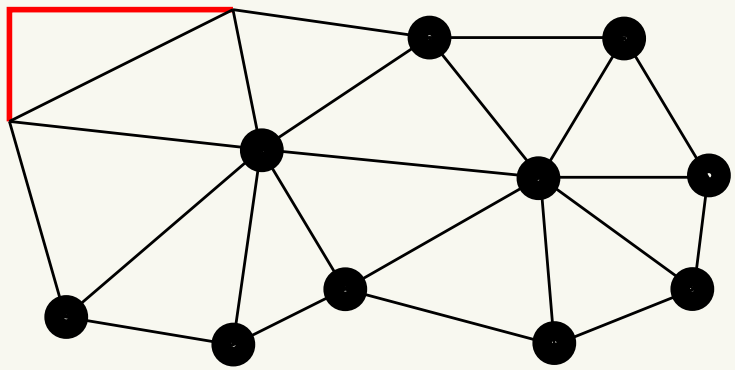

On the other hand, if the set of edges where functions in V_h vanish is too small, then $V_h \not\subset V$.

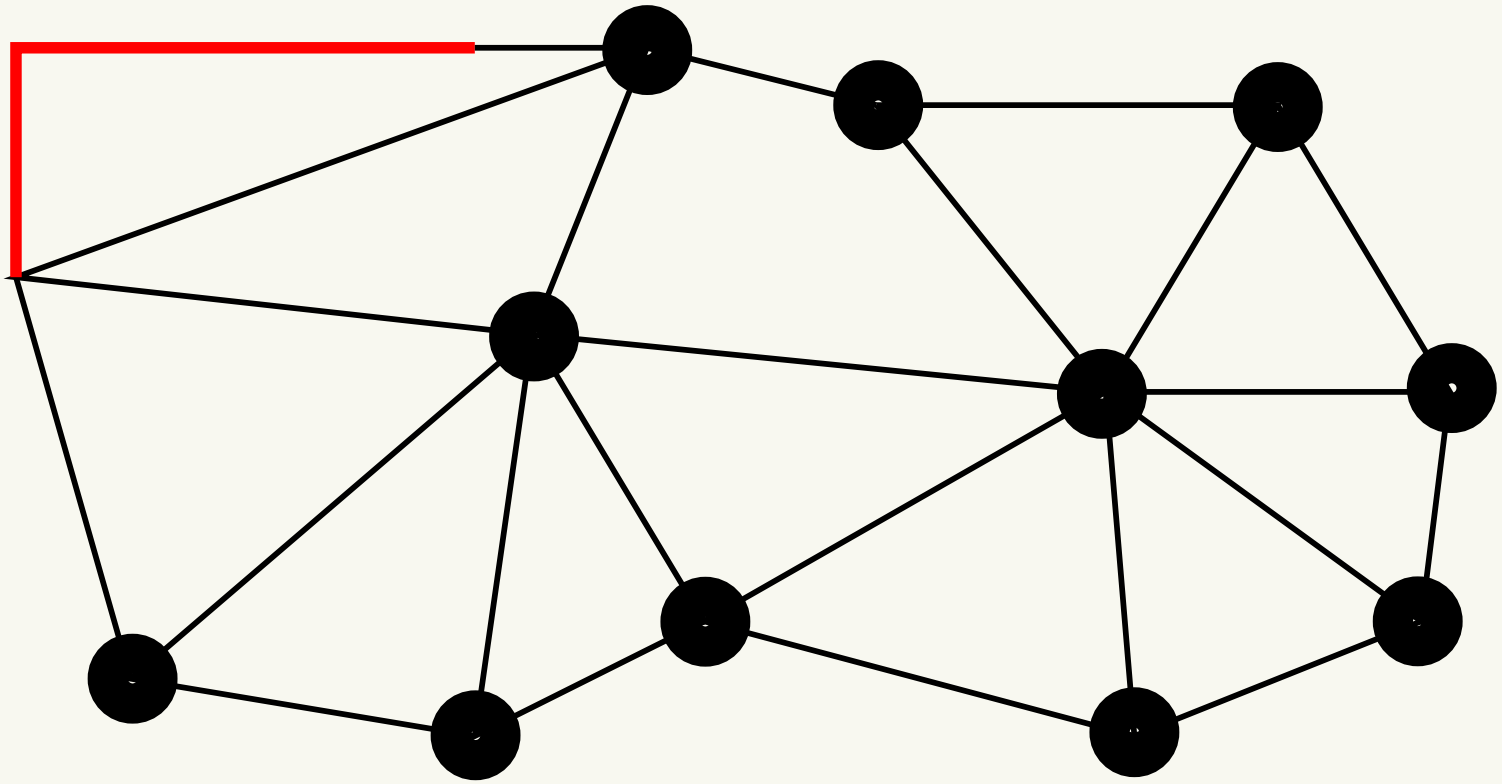

If the set of edges where functions in V_h vanish

is too big, then (28) ($I_h\left(V \cap C^k(\Omega)\right) \subset V_h$) fails to hold.

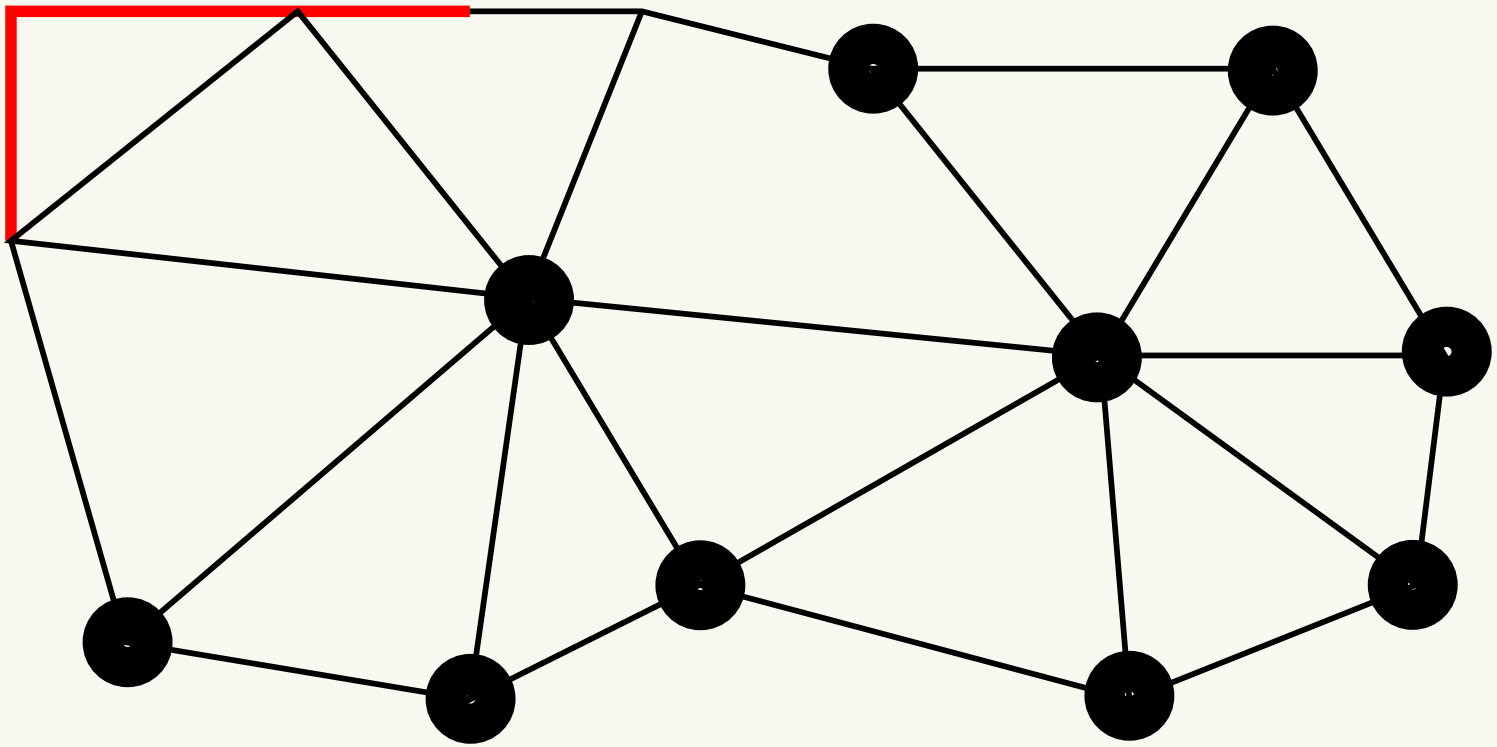

Matching Boundary Conditions

In the case of pure Dirichlet data, i.e., $\Gamma = \partial\Omega$, then V_h is just the set of piecewise polynomials that vanish on the entire boundary.

In the case of pure Neumann data, i.e., $\Gamma = \emptyset$, V_h is the entire set of piecewise polynomials with no constraints at the boundary.

Even if finite element space matches Γ correctly, there is a singularity associated with changing boundary condition type along a straight boundary.

Estimates in other norms

Frequently, it is the case that the $L^2(\Omega)$ norm is better by one power of h:

$$\|u - u_h\|_{L^2(\Omega)} \leq Ch^m |u|_{H^m(\Omega)}. \tag{29}$$

This follows by a duality relationship.

Denote the error $e_h = u - u_h$.

We solve Poisson's problem with e_h as the data:

$$a(\phi, v) = (e_h, v)_{L^2(\Omega)} \quad \forall v \in V.$$

Then we have an expression for $\|e_h\|_{L^2(\Omega)}$:

$$\|e_h\|^2_{L^2(\Omega)} = (e_h, e_h)_{L^2(\Omega)} = a(\phi, e_h).$$

Subtracting the variational formulations for u and u_h, we find $a(e_h, v) = 0$ for all $v \in V_h$, so

$$\|e_h\|^2_{L^2(\Omega)} = a(\phi - v, e_h)$$

for all $v \in V_h$. Choosing v appropriately, we find

$$\|e_h\|^2_{L^2(\Omega)} \leq Ch\|\phi\|_{H^2(\Omega)}\|e_h\|_{H^1(\Omega)}. \tag{30}$$

For smooth problems,

$$\|\phi\|_{H^2(\Omega)} \leq C\|e_h\|_{L^2(\Omega)}, \tag{31}$$

so we conclude that

$$\|e_h\|^2_{L^2(\Omega)} \leq Ch\|e_h\|_{L^2(\Omega)}\|e_h\|_{H^1(\Omega)}.$$

Duality result

Dividing by $\|e_h\|_{L^2(\Omega)}$, we find

$$\|e_h\|_{L^2(\Omega)} \leq Ch\|e_h\|_{H^1(\Omega)}.$$

This proves (29) provided (31) holds.

As we will see, latter is not always the case.

Since Galerkin is a least-squares method, we might not expect errors to behave well uniformly.

Might not be surprising that errors near the boundary would be slightly worse but in a small region.

Significant that this is not generally the case.

L^∞ estimates

Rather, it is possible to prove that $\|u - u_h\|_{W^1_\infty(\Omega)}$ and $\|u - u_h\|_{H^1(\Omega)}$ are of the same order of accuracy in h.

Similarly, $\|u - u_h\|_{L^2(\Omega)}$ and $\|u - u_h\|_{L^\infty(\Omega)}$ are of the same order of accuracy in h, with one small exception.

With piecewise linear approximation, $\|u - u_h\|_{L^\infty(\Omega)}$ can be worse by a factor of $|\log h|$ than $\|u - u_h\|_{L^2(\Omega)}$.

Uniform bounds for FEM are much complex to prove than duality argument used to prove L^2 estimates.

But they have been extended to many complicated systems such as the Navier-Stokes equations.

A reality check

Error estimates provide check on code performance.

For example, if we consider two meshes, of size h and $h/2$, then we expect that

$$\|u - u_h\|_{H^1(\Omega)} / \|u - u_{h/2}\|_{H^1(\Omega)} \approx h^{m-1}/(h/2)^{m-1} = 2^{m-1}.$$

Thus we would have

$$m - 1 = \log_2 \left(\|u - u_h\|_{H^1(\Omega)} / \|u - u_{h/2}\|_{H^1(\Omega)} \right).$$

Similarly, if (29) holds, we have

$$\|u - u_h\|_{L^2(\Omega)} / \|u - u_{h/2}\|_{L^2(\Omega)} \approx h^m/(h/2)^m = 2^m.$$

Empirical rate

Thus we define the quantity “rate” in Table 4 via

$$\text{rate} = \log_2 \left(\|u - u_h\|_{L^2(\Omega)} / \|u - u_{h/2}\|_{L^2(\Omega)} \right). \tag{32}$$

Recall that we expect $m \approx k + 1$ where k is the degree of piecewise polynomials used for the simulation.

Of course, this is only a “not to exceed” rate, so your experience may differ.

In fact, the observed rate can be negative, due to round-off error amplification via the condition number of the system.

Varying variational formulations

Review: variational formulations can be used for

- a language for PDEs
- basis for PDE theory
- foundation for numerical approximation.

Ingredients for a variational formulation:

- the variational space V
- the bilinear form $a(\cdot, \cdot)$
- a linear functional F (data for the problem).

We have seen how V can change via the Neumann problem.

Now we consider other changes.

Inhomogeneous Boundary Conditions: varying F

When boundary conditions are equal to zero, we often call them homogeneous, whereas we refer to nonzero boundary conditions as inhomogeneous.

Inhomogeneous boundary conditions are easily treated.

For example, suppose that we wish to solve (1) with boundary conditions

$$u = g_D \text{ on } \Gamma \subset \partial\Omega \qquad \text{and} \qquad \frac{\partial u}{\partial n} = g_N \text{ on } \partial\Omega \backslash \Gamma, \quad (33)$$

where g_D and g_N are given.

For simplicity, let us assume that g_D is defined on all of Ω, with $g_D \in H^1(\Omega)$ and that $g_N \in L^2(\partial\Omega\backslash\Gamma)$.

Well-posedness of inhomogeneous formulation

Recall the space (3): $V = \left\{ v \in H^1(\Omega) \ : \ v|_\Gamma = 0 \right\}$.

Then the variational formulation of (1) , (33) is as follows: find u such that $u - g_D \in V$ and such that

$$a(u, v) = (f, v)_{L^2(\Omega)} + \oint_{\partial\Omega\setminus\Gamma} g_N v \, ds \quad \forall v \in V. \tag{34}$$

This is well-posed since the linear form

$$F(v) := (f, v)_{L^2(\Omega)} + \oint_{\partial\Omega\setminus\Gamma} g_N v \, ds$$

is well defined (and continuous) for all $v \in V$.

Inhomogeneous BCs: finite element formulation

Finite element approximation of (34) involves, typically, use of an interpolant, $I_h g_D$, of the Dirichlet data.

Seek u_h such that $u_h - I_h g_D \in V_h$ and

$$a(u_h, v) = (f, v)_{L^2(\Omega)} + \oint_{\partial\Omega\setminus\Gamma} g_N v \, ds \quad \forall v \in V_h. \tag{35}$$

We can cast this in a more standard form as: find $\hat{u}_h = u_h - I_h g_D \in V_h$ such that

$$a(\hat{u}_h, v) = (f, v)_{L^2(\Omega)} + \oint_{\partial\Omega\setminus\Gamma} g_N v \, ds - a(I_h g_D, v) \quad \forall v \in V_h.$$

Then we can set $u_h = \hat{u}_h + I_h g_D$.

The `dolfin` built-in function `solve` automates this, so data g_D just needs to be specified.

Define the affine space $V + g_D$ by

$$V + g_D = \{v + g_D \ : \ v \in V\}\,.$$

Affine variational formulation: find $u \in V + g_D$ such that

$$a(u, v) = (f, v)_{L^2(\Omega)} + \oint_{\partial\Omega\setminus\Gamma} g_N v \, ds \quad \forall v \in V.$$

Discrete approximation: Find $u_h \in V_h + I_h g_D$ such that

$$a(u_h, v) = (f, v)_{L^2(\Omega)} + \oint_{\partial\Omega\setminus\Gamma} g_N v \, ds \quad \forall v \in V_h.$$

Affine variational formulation

Original variational formulation has three ingredients: space V, bilinear form $a(\cdot, \cdot)$ and linear form data $F(\cdot)$.

Affine variational formulation has four ingredients: V, $a(\cdot, \cdot)$, $F(\cdot)$, **and** the Dirichlet data function g_D.

Simplifies formulation of many PDE problems.

Fortunately, the `dolfin` built-in function `solve` automates all of this.

Dirichlet data function g_D needs to be specified just in the call to `solve`.

Modification interlude

Here are the modifications seen so far.

Pure Neumann boundary conditions modified variational space V.

Inhomogeneous boundary conditions

- Natural: modification in right-hand side F.
- Essential: affine variational formulation.

Now we look at a case where the variational form changes.

Robin boundary conditions: varying $a(\cdot, \cdot)$

It is frequently the case that more complex boundary conditions arise in physical models.

The so-called Robin boundary conditions take the form

$$\alpha u + \frac{\partial u}{\partial n} = 0 \text{ on } \partial\Omega \backslash \Gamma, \tag{36}$$

where α is a positive measurable function.

This will be coupled as before with a Dirichlet condition on Γ.

A variational formulation for this problem can be derived as follows.

Robin variational problem

Let V be the space defined in (3) with the added proviso that $V = H^1(\Omega)$ in the case that $\Gamma = \emptyset$.

From (5), we get

$$\begin{aligned}(f, v)_{L^2(\Omega)} &= \int_\Omega (-\Delta u(\mathbf{x}))v(\mathbf{x})\, d\mathbf{x} \\ &= \int_\Omega \nabla u(\mathbf{x}) \cdot \nabla v(\mathbf{x})\, d\mathbf{x} - \oint_{\partial\Omega} v(s)\frac{\partial u}{\partial n}(s)\, ds \\ &= \int_\Omega \nabla u(\mathbf{x}) \cdot \nabla v(\mathbf{x})\, d\mathbf{x} + \oint_{\partial\Omega} \alpha(s)\, v(s)\, u(s)\, ds,\end{aligned}$$

after substituting the boundary condition $\frac{\partial u}{\partial n} = -\alpha u$ on $\partial\Omega\backslash\Gamma$ and using the condition (3) that $v = 0$ on Γ.

Robin variational form

Thus we define a new variational form

$$a_{\text{Robin}}(u,v) := \int_\Omega \nabla u(\mathbf{x}) \cdot \nabla v(\mathbf{x})\, d\mathbf{x} + \oint_{\partial\Omega} \alpha(s)\, v(s)\, u(s)\, ds.$$

Variational formulation for the equation (1) together with the Robin boundary condition (36) takes the usual form

$$u \in V \quad \text{satisfies} \quad a_{\text{Robin}}(u,v) = (f,v)_{L^2(\Omega)} \quad \forall v \in V. \quad (37)$$

A solution to the variational problem (37) solves both (1) and (36) under suitable smoothness conditions.

Robin variational form coercivity

Note that $a_{\text{Robin}}(\cdot,\cdot)$ is coercive on $H^1(\Omega)$, that is there is a constant $C < \infty$ such that

$$\|v\|^2_{H^1(\Omega)} \leq C a_{\text{Robin}}(v,v) \quad \forall v \in H^1(\Omega).$$

This holds even if $\Gamma = \emptyset$.

Coercivity follows because $\alpha > 0$:

$$a_{\text{Robin}}(v,v) = a(v,v) + \oint_{\partial\Omega} \alpha(s)\, v(s)^2\, ds.$$

(Proof is a Sobolev space exercise.)

If α were negative, it might not be coercive.

We have seen modifications to all 3 components of the variational problem.

Now we consider how the problem domain impacts the solution.

Sobolev spaces are essential to characterize solutions.

Geometry matters: varying the domain Ω

The geometry of the domain boundary has a significant impact on the regularity of the solution.

We begin by considering the problem

$$\begin{aligned} -\Delta u &= 0 \text{ in } \Omega \\ u &= g \text{ on } \partial\Omega, \end{aligned} \tag{38}$$

where Ω is a polygonal domain in $\mathbb{R}^2$.

We will see that the principal singularity of the solution can be identified, associated with what are often called re-entrant vertices.

L-shaped domain

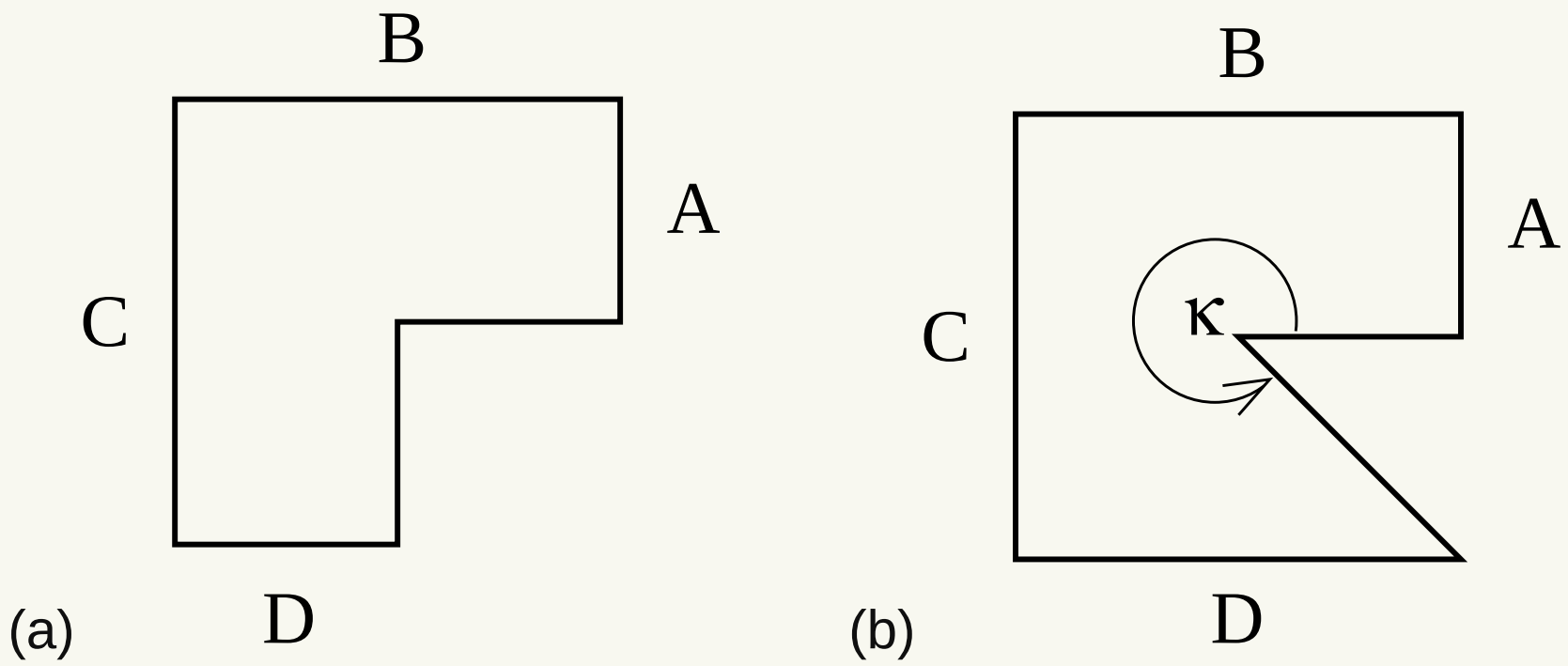

Figure 9: (a) L-shaped domain, (b) re-entrant corner of angle κ.

The **L-shaped** domain Ω is depicted in Figure 9(a):

$$\Omega = [-1,1]^2 \cap \left\{ (x,y) = (r\cos\theta, r\sin\theta) \ : \ 0 \leq r, \ 0 < \theta < \tfrac{3}{2}\pi \right\},$$

defined using polar coordinates $(x,y) = r(\cos\theta, \sin\theta)$.

Re-entrant corners

Again using polar coordinates, define

$$g(r(\cos\theta, \sin\theta)) = r^{2/3}\sin(\tfrac{2}{3}\theta). \tag{39}$$

$\partial\Omega$ has two parts: the convex part $\Gamma_c = A \cup B \cup C \cup D$ where

$$A = \{(1, y) \ : \ 0 \le y \le 1\}, \qquad B = \{(x, 1) \ : \ -1 \le x \le 1\},$$
$$C = \{(-1, y) \ : \ -1 \le y \le 1\}, \quad D = \{(x, -1) \ : \ 0 \le x \le 1\},$$

(see Figure 9) and the re-entrant part

$$\Gamma_r = \{(0, y) \ : \ -1 \le y \le 0\} \cup \{(x, 0) \ : \ 0 \le x \le 1\}.$$

Then our data $g = 0$ on Γ_r. Moreover, g is **harmonic**, meaning $\Delta g = 0$.

This follows immediately from complex analysis, since g is the imaginary part of the complex analytic function $e^{(2/3)z}$.

Deriving such a result is not easy using calculus.
First of all, using polar coordinates $(x, y) = r(\cos\theta, \sin\theta)$, we find

$$\nabla r = \frac{(x,y)}{r} \quad \text{and} \quad \nabla\theta = \frac{(-y,x)}{r^2}. \quad \text{This means that}$$

$$\begin{aligned}
\nabla g(x,y) &= \tfrac{2}{3}\big((\nabla r) r^{-1/3}\sin(\tfrac{2}{3}\theta) + (\nabla\theta) r^{2/3}\cos(\tfrac{2}{3}\theta)\big) \\
&= \tfrac{2}{3} r^{-4/3}\big((x,y)\sin(\tfrac{2}{3}\theta) + (-y,x)\cos(\tfrac{2}{3}\theta)\big) \\
&= \tfrac{2}{3} r^{-4/3}\big(x\sin(\tfrac{2}{3}\theta) - y\cos(\tfrac{2}{3}\theta), y\sin(\tfrac{2}{3}\theta) + x\cos(\tfrac{2}{3}\theta)\big) \\
&= \tfrac{2}{3} r^{-1/3}\big(-\sin(\tfrac{1}{3}\theta), \cos(\tfrac{1}{3}\theta)\big),
\end{aligned} \tag{40}$$

where trigonometric identities flow from the expressions ($\iota = \sqrt{-1}$)

$$\begin{aligned}
&\cos(\tfrac{1}{3}\theta) - \iota\sin(\tfrac{1}{3}\theta) = \cos(-\tfrac{1}{3}\theta) + \iota\sin(-\tfrac{1}{3}\theta) = e^{-\iota(1/3)\theta} = e^{-\iota\theta} e^{\iota(2/3)\theta} \\
&= \big(\cos\theta - \iota\sin\theta\big)\big(\cos(\tfrac{2}{3}\theta) + \iota\sin(\tfrac{2}{3}\theta)\big) \\
&= \big(\cos\theta\cos(\tfrac{2}{3}\theta) + \sin\theta\sin(\tfrac{2}{3}\theta)\big) + \iota\big(-\sin\theta\cos(\tfrac{2}{3}\theta) + \cos\theta\sin(\tfrac{2}{3}\theta)\big).
\end{aligned}$$

Gradient unbounded

The immediate result of the calculation (40) is that, for $0 < \theta < \frac{3}{2}\pi$,

$|\nabla g(x, y)|$ blows up like $|(x, y)|^{-1/3}$, since

$$|\nabla g(x, y)| = |\nabla g(r\cos\theta, r\sin\theta)| = \tfrac{2}{3}r^{-1/3} = \tfrac{2}{3}|(x, y)|^{-1/3}.$$

Therefore $|\nabla g(x, y)|$ is square integrable, but it is obviously not bounded.

Benefit of working with Sobolev spaces:

allows g to be considered a reasonable function

even though it has an infinite gradient.

Gradient unbounded

We can in principle use the vector calculus identity

$$\nabla\cdot(\phi\boldsymbol{\psi}) = \nabla\phi\cdot\boldsymbol{\psi} + \phi\nabla\cdot\boldsymbol{\psi}$$

to compute

$$\Delta g = \nabla\cdot(\nabla g)$$

to verify that $\Delta g = 0$, but the algebra is daunting.

Exercise: compute solution via variational problem (35), see if $u = g$ throughout Ω.

Another exercise: verify that $\Delta g = 0$ analytically using polar coordinates.

General non-convex domains

Singularity like the L-shaped domain occurs for any domain with **non-convex vertex** depicted in Figure 9(b), where the angle of the **re-entrant vertex** is κ.

The L-shaped domain corresponds to $\kappa = \frac{3}{2}\pi$.

The principle singularity for such a domain is of the form

$$g_\kappa(r(\cos\theta, \sin\theta)) = r^{\pi/\kappa}\sin((\pi/\kappa)\theta). \tag{41}$$

Note that when $\kappa < \pi$ (a convex vertex), the gradient of g_κ is bounded.

Exercise: explore this general case for various values of κ.

Slit domain

The largest that κ can be is 2π which corresponds to a **slit domain**.

We have $g_{2\pi} = \sqrt{r}\sin(\frac{1}{2}\theta)$, which is still in $H^1(\Omega)$.

The slit domain is often a model for **crack propagation**.

An illustration of a problem on a slit domain is given by

$$\begin{aligned} -\Delta u &= 1 \text{ in } [0,1]\times[-1,1] \\ u = 0 \text{ on } \Gamma, \quad \frac{\partial u}{\partial n} &= 0 \text{ on } \partial\Omega\backslash\Gamma, \end{aligned} \tag{42}$$

where $\Gamma = \left\{(x,0) \ : \ x \in [\frac{1}{2},1]\right\}$.

Slit domain continued

The solution of (42) is depicted in Figure 10, where only the top half of the domain (that is, $[0, 1] \times [0, 1]$) is shown.

The solution in the bottom half of the domain can be obtained by symmetric reflection across the x-axis.

The square-root singularity is clearly visible.

Slit domain solution

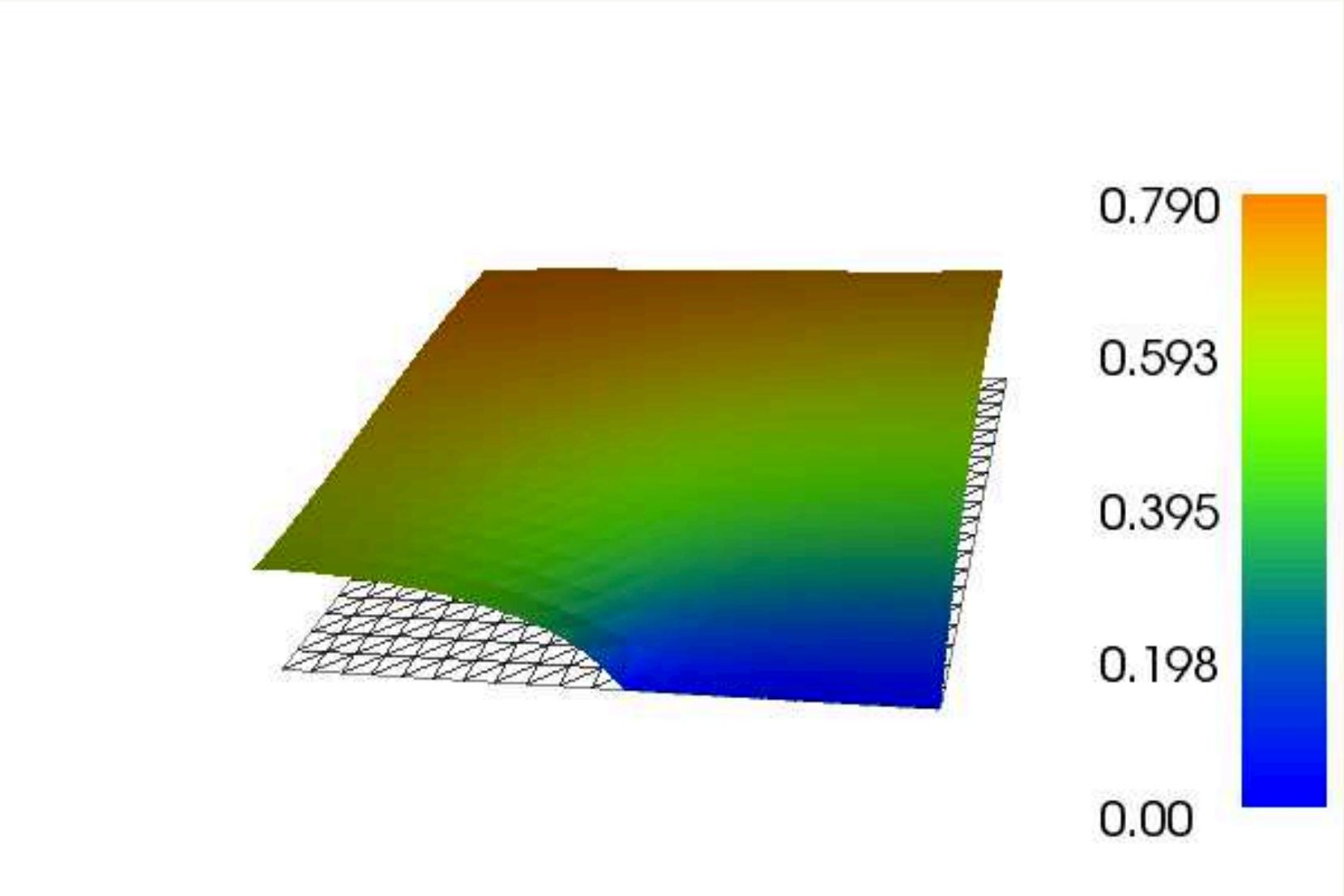

Figure 10: Illustration of the singularity that can occur when boundary condition types are changed, cf. (43), as well as a cut-away of the solution to slit problem (42). Computed with piecewise linears on the indicated mesh.

General non-convex domains

The range of κ values for a realistic polygonal domain excludes a region around $\kappa = 0$ and $\kappa = \pi$.

In particular, we see that $\kappa = \pi$ does not yield a singularity; the boundary is a straight line in this case, and $g_\pi(x, y) = r \sin\theta = y$, which is not singular.

When $\kappa = 0$, there is no interior in the domain near this point.

Thus for any polygonal domain with a finite number of vertices with angles κ_j, there is some $\epsilon > 0$ such that

$$\kappa_j \in [\epsilon, \pi - \epsilon] \cup [\pi + \epsilon, 2\pi] \text{ for all } j.$$

Three-dimensional singularities

In three dimensions, the set of possible singularities is much greater [4].

Edge singularities correspond to the vertex singularities in two dimensions, but in addition, vertex singularities appear [10].

The effect of smoothing singular boundaries is considered in [6].

Changing boundary condition type

When boundary conditions change type along a straight line, singularity same as slit domain.

Suppose that we have a domain

$$\Omega = \left\{(x, y) \in \mathbb{R}^2 \ : \ x \in [-1, 1], \ y \in [0, 1]\right\}$$

and we impose homogeneous Dirichlet conditions on

$$\Gamma = \left\{(x, 0) \in \mathbb{R}^2 \ : \ x \in [0, 1]\right\}$$

and Neumann conditions on $\partial\Omega \backslash \Gamma$.

We can reflect the domain Ω around the line $y = 0$, and we get the domain $[-1, 1]^2$ with a slit given by Γ.

Reflected solution is slit solution

$g_{2\pi} = \sqrt{r}\sin(\frac{1}{2}\theta)$ satisfies Dirichlet conditions on Γ and Neumann conditions on Γ^*.

Such singularities occur any time we switch from Dirichlet to Neumann boundary conditions along a straight boundary segment.

We illustrate this with the following problem:

$$\begin{aligned} -\Delta u &= 1 \text{ in } [0,1]^2 \\ u = 0 \text{ on } \Gamma, \quad \frac{\partial u}{\partial n} &= 0 \text{ on } \partial\Omega\backslash\Gamma, \end{aligned} \tag{43}$$

where $\Gamma = \left\{(x,0) \ : \ x \in [\frac{1}{2},1]\right\}$, cf. Figure 10.

Exercise: explore this problem in more detail.

Same picture as for the slit domain

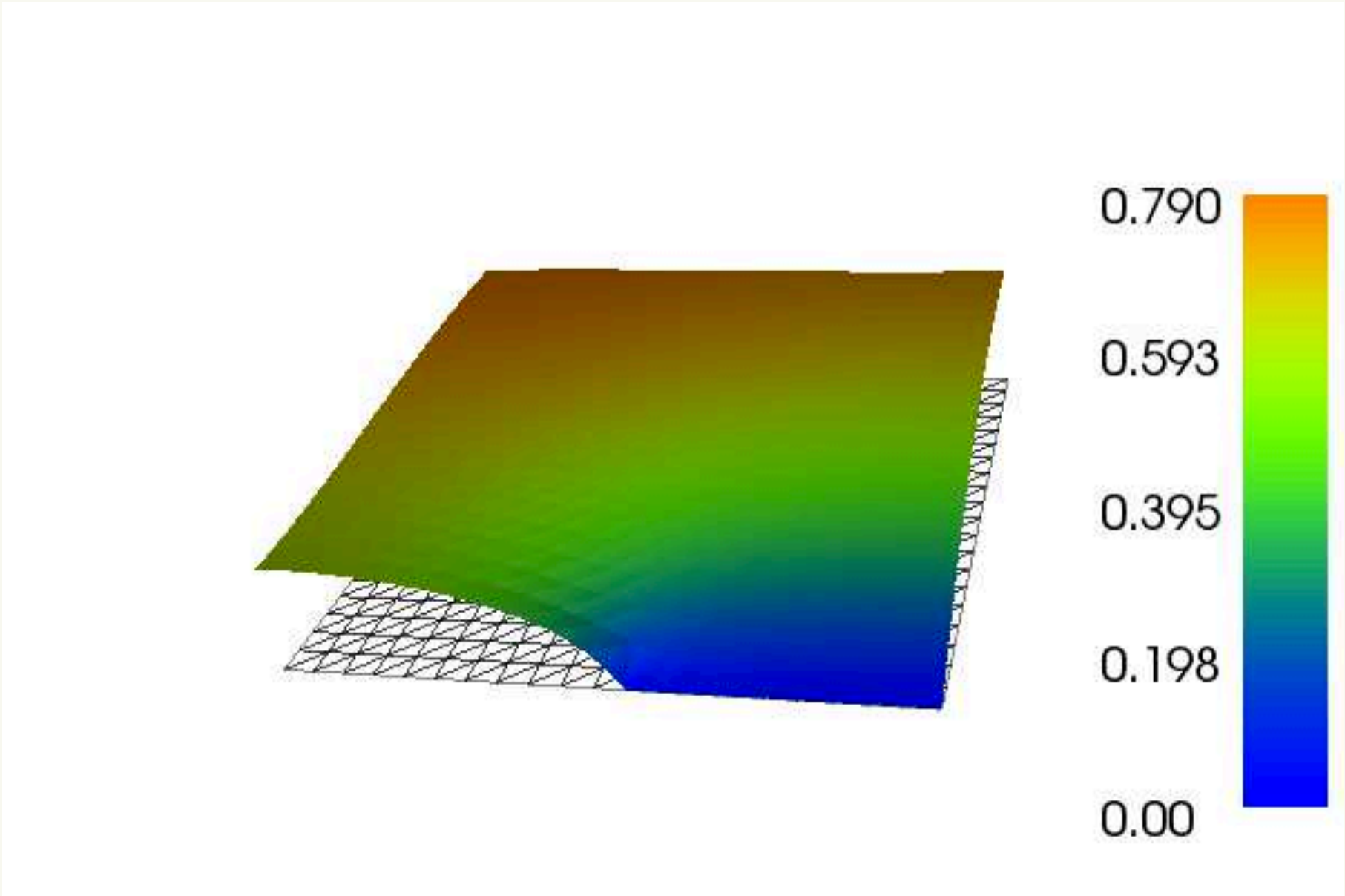

Now consider a modeling challenge:

what is shape of drum head

if you push down on it

with a sharp pin?

We will see that the appropriate model is not obvious.

Localized behavior

How to model localized behavior in a physical system?

Tempting to model as an effect occuring at a single point.

The Laplace equation models (to a reasonable extent) deformation of the drum head (for small deformations).

So one might consider

$$-\Delta u = 0 \text{ in } \Omega$$
$$u(\mathbf{x}_0) = u_0$$

where u_0 denotes the prescribed position of the pencil.

An ill-posed problem?

However, this problem is not well posed.

Difficulty: one cannot constrain a function in $H^1(\Omega)$ at a single point.

This is illustrated by the function [2, Example 1.4.3]

$$v(\mathbf{x}) = \log|\log|\mathbf{x}||\tag{44}$$

which satsifies $v \in H^1(B)$ where

$$B = \left\{\mathbf{x} \in \mathbb{R}^2 \ : \ |\mathbf{x}| < \tfrac{1}{2}\right\}.$$

This function does not have a well-defined point value at the origin.

Knife edge versus pin

Thus setting a point value for a function in H^1 does not make sense.

By shifting this function around, we realize that functions in H^1 may not have point values on a dense set of points $\{\mathbf{x}_i\}$:

$$u(\mathbf{x}) = \sum_{i=1}^{\infty} 2^{-i} \log|\log|\mathbf{x} - \mathbf{x}_i||$$

For example, take the set of points $\{\mathbf{x}_i\}$ to be dense in

$$D = \left\{\mathbf{x} \in \mathbb{R}^2 \ : \ |\mathbf{x}| < \tfrac{1}{4}\right\}.$$

Knife edge versus pin

It is possible to change to a Dirichlet problem

$$-\Delta u = 0 \text{ in } \Omega$$
$$u = u_0 \text{ on } \Gamma$$

where Γ is a small curve representing the point of contact of a knife edge with the drum head, and u_0 is some function defined on Γ.

As long as Γ has positive length, this problem is well posed.

However, its behavior will degenerate as the length of Γ is decreased.

Fundamental solution

Another approach to modeling such phenomena is using the Dirac δ-function [2]:

$$\begin{aligned} -\Delta u &= \delta_{\mathbf{x}_0} \text{ in } \Omega \\ u &= 0 \text{ on } \partial\Omega, \end{aligned} \tag{45}$$

where $\delta_{\mathbf{x}_0}$ is the linear functional $\delta_{\mathbf{x}_0}(v) = v(\mathbf{x}_0)$.

Again, there is an issue since this linear functional is not bounded on V, as the function v defined in (44) illustrates.

On the other hand, the solution to (45) is known as the Green's function for the Laplacian on Ω (with Dirichlet conditions).

Possible to make sense of (45) using sophisticated Sobolev spaces [2].

However, rather than taking that approach, we take one that effectively resolves the issue in conventional spaces.

What we do is replace $\delta_{\mathbf{x}_0}$ by a smooth function $\delta^A_{\mathbf{x}_0}$ with the property that

$$\int_\Omega \delta^A_{\mathbf{x}_0}(\mathbf{x})\, v(\mathbf{x})\, d\mathbf{x} \to v(\mathbf{x}_0) \text{ as } A \to \infty$$

for sufficiently smooth v.

Mollified $\delta_{\mathbf{x}_0}$

We then consider the problem

$$\begin{aligned} \Delta u^A &= \delta^A_{\mathbf{x}_0} \text{ in } \Omega \\ u^A &= g \text{ on } \partial\Omega. \end{aligned} \tag{46}$$

Note that we can pick g to be the fundamental solution, and thus we have $u^A \to g$ as $A \to \infty$.

For example, we can choose $\delta^A_{\mathbf{x}_0}$ to be Gaussian function of amplitude A and integral 1. In particular, in two dimensions,

$$\delta^A_{\mathbf{x}_0} = A\, e^{-\pi A|\mathbf{x}-\mathbf{x}_0|^2}.$$

Sanity check

We check our requirement that the integral is 1 via the change of variables $\mathbf{y} = \sqrt{\pi A}\,\mathbf{x}$:

$$\begin{aligned}\int_{\mathbb{R}^2} \pi A\, e^{-\pi A|\mathbf{x}-\mathbf{x}_0|^2}\, d\mathbf{x} &= \int_{\mathbb{R}^2} e^{-|\mathbf{y}-\mathbf{y}_0|^2}\, d\mathbf{y} \\ &= 2\pi \int_0^\infty e^{-r^2} r\, dr \\ &= \pi \int_0^\infty e^{-s}\, ds = \pi.\end{aligned}$$

In our experiments, $\mathbf{x}_0$ was chosen to be near the middle of the square $\Omega = [0,1]^2$, that is, $\mathbf{x}_0 = (0.50001, 0.50002)$ to avoid having the singularity at a grid point.

Manufactured solution

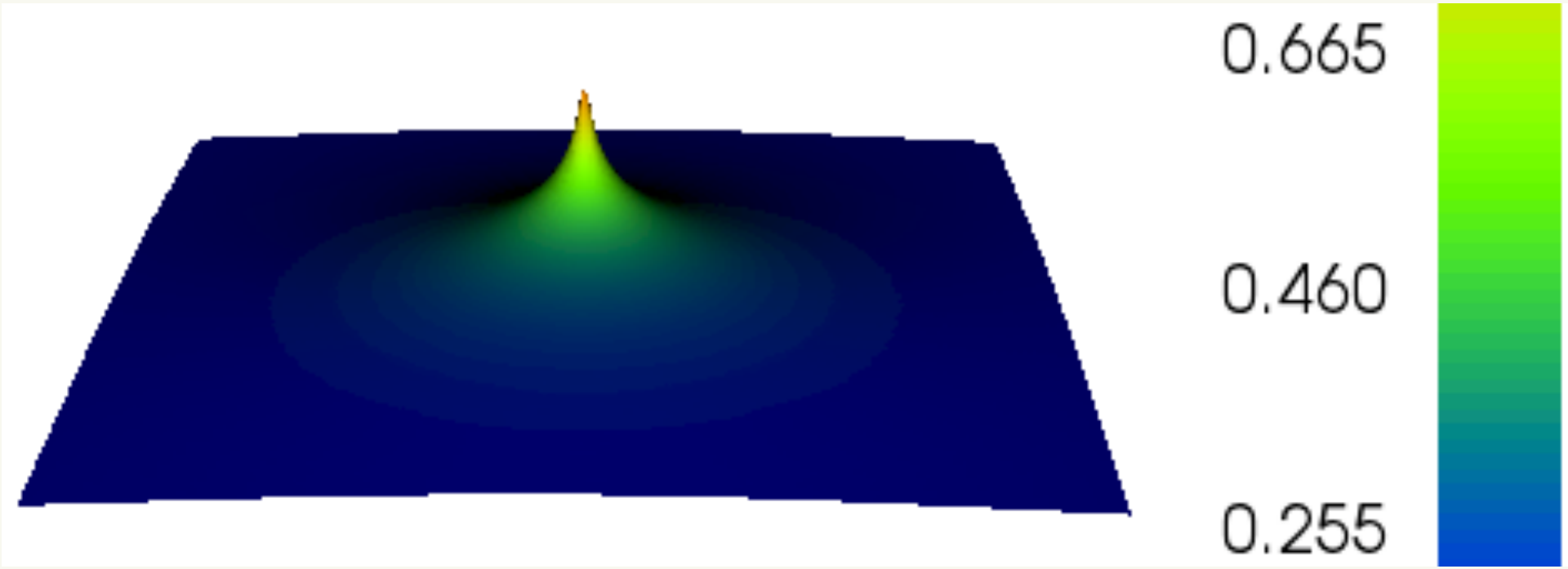

Figure 11: Solution of (46) computed with a mesh size of 512 with piecewise linears and $A = 10,000$.

Manufactured solution

The fundamental solution for the Laplace equation in two dimensions is

$$g(\mathbf{x}) = -\frac{1}{2\pi} \log |\mathbf{x} - \mathbf{x}_0|,$$

and so we took as boundary conditions $g(\mathbf{x})$ for $\mathbf{x} \in \partial\Omega$.

Approximation of singular Green's function only first order accurate.

Increasing the order of polynomials used is only of modest benefit.

Increasing the amplitude of the approximate δ-function useful up to a point, but making it larger only of value if the mesh is refined.

degree	mesh	amplitude	error	check-sum
1	128	10,000	5.27e-03	-2.34e-02
1	256	10,000	2.50e-03	-4.57e-09
1	512	10,000	1.47e-03	-2.22e-16
1	1024	10,000	1.08e-03	5.11e-15
4	256	10,000	9.73e-04	-1.02e-10
1	512	100,000	9.67e-04	-1.06e-03
1	1024	100,000	5.24e-04	-1.98e-14

Table 5: Data for the solution of (46). Key: degree is the degree of polynomials used, mesh is the number of triangle pairs in each direction. The amplitude is A, error is $\|u_h^A - g\|_{L^2(\Omega)}$, check-sum is the value $1 - \int_\Omega \left(\delta_{\mathbf{x}_0}^A\right)_h d\mathbf{x}$ where $\left(\delta_{\mathbf{x}_0}^A\right)_h$ denotes the interpolant of $\delta_{\mathbf{x}_0}^A$ in V_h.

Mismatch in boundary conditions yields singularity

A mismatch between boundary conditions can lead to a singularity.

Consider the boundary value problem

$$\begin{aligned} -\Delta u &= 0 \text{ in } \Omega \\ u &= 0 \text{ on } \Gamma \\ \frac{\partial u}{\partial n} &= g \text{ on } \Omega \backslash \Gamma, \end{aligned} \tag{47}$$

where $\Omega = [0,1]^2$, $g(y) = 1$ and

$$\Gamma = \{(x,y) \in \partial\Omega \ : \ x = 0 \text{ or } y = 0 \text{ or } y = 1\}.$$

Mismatch in boundary conditions

Thus $\Omega \backslash \Gamma = \{(x, y) \in \partial\Omega \ : \ x = 1\}$.

Define $\Gamma_0 = \{(x, y) \in \partial\Omega \ : \ y = 0$ or $y = 1\} \subset \Gamma$.

Since $u \equiv 0$ on Γ, it follows that $\frac{\partial u}{\partial x} = 0$ on Γ_0,

But $\frac{\partial u}{\partial x} = 1$ on $\Omega \backslash \Gamma$, so there is a discontinuity in $\frac{\partial u}{\partial x}$ at $(1, 0)$ and $(1, 1)$.

In particular, second derivatives of u blow up like r^{-1} where r is the distance to $(1, 0)$ or $(1, 1)$.

Thus $u \notin H^2(\Omega)$.

Viz technique

To visualize this phenomenon, we have plotted $\frac{\partial u}{\partial x}$ in Figure 12.

As expected, $\frac{\partial u}{\partial x} = 0$ on Γ, and $\frac{\partial u}{\partial x} = 1$ on $\Omega \backslash \Gamma$ away from the singular points $(1, 0)$ or $(1, 1)$.

At these points, the approximation can exhibit unpredictable behavior for some meshes.

The code used to compute $\frac{\partial u}{\partial x}$ is

```
v=grad(u)[0]
```

Mismatch plot

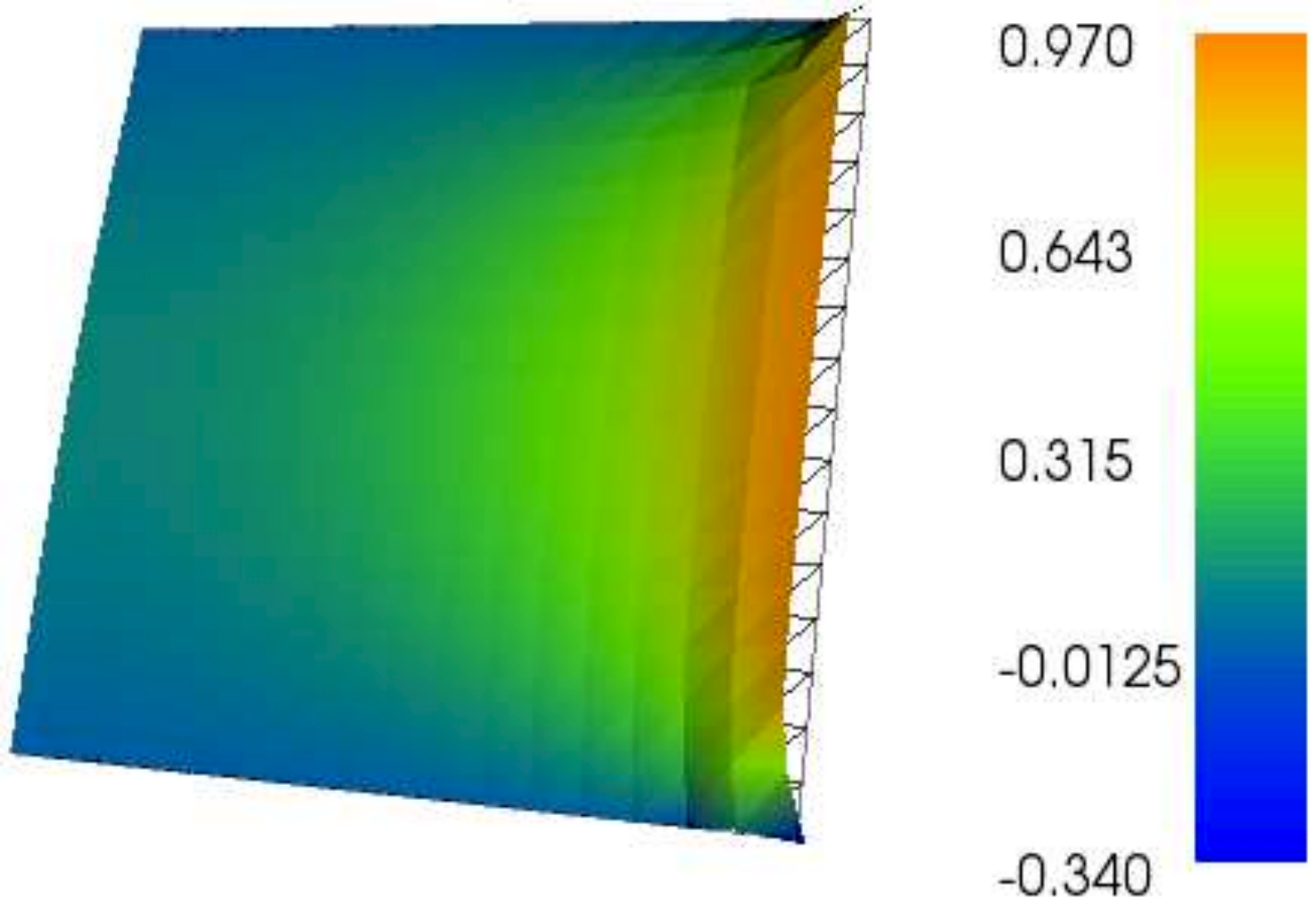

Figure 12: Plot of $\frac{\partial u}{\partial x}$ where u is the solution of (47) approximated with piecewise linears on a 16×16 mesh. We see that $\frac{\partial u}{\partial x} = 0$ on Γ_0 (top and bottom sides of $\Omega = [0,1]^2$) and $\frac{\partial u}{\partial x} = 1$ on $\partial\Omega \backslash \Gamma$ (right side of $\Omega = [0,1]^2$).

Modifying the equation

So far, everything has been based on the Laplace/Poisson equation

Now we modify the PDE itself.

Simplest modification: add a potential.

Let’s see what the issues are!

Adding a potential

We now augment the equation (1) with a potential Z, which is simply a function defined on Ω with real values. The PDE takes the form

$$-\Delta u + Zu = f \text{ in } \Omega \tag{48}$$

together with the boundary conditions (2).

To formulate the variational equivalent of (1) with boundary conditions (2), we again use the variational space

$$V := \left\{ v \in H^1(\Omega) \ : \ v|_\Gamma = 0 \right\}.$$

The appropriate bilinear form for the variational problem is then

$$a_Z(u,v) = \int_\Omega \nabla u(\mathbf{x}) \cdot \nabla v(\mathbf{x}) + Z(\mathbf{x}) u(\mathbf{x}) v(\mathbf{x})\, d\mathbf{x}.$$

In the case of homogeneous boundary conditions, we seek a solution $u \in V$ to

$$a_Z(u,v) = \int_\Omega f(\mathbf{x}) v(\mathbf{x})\, d\mathbf{x} \quad \forall\, v \in V. \tag{49}$$

The simplest case is when Z is a constant, in which case (48) is often called the **Helmholtz equation**.

Bounded V

The Helmholtz problem becomes interesting if Z is large, or equivalently, there is a small coefficient in front of Δ in (48).
Exercise: explore this problem.

To understand coercivity in such problems, we first consider the eigenvalue problem

$$-\Delta u = \lambda u \text{ in } \Omega \tag{50}$$

together with the boundary conditions (2).

Denote solution of (50) by u_λ.

Potential coercivity

Let λ_0 be the lowest eigenvalue, and $u_{\lambda_0} \in V$ the corresponding eigenvector, for the eigenproblem problem (50):

$$a_0(u_\lambda, v) = \lambda \int_\Omega u_\lambda(\mathbf{x}) v(\mathbf{x})\, d\mathbf{x} \quad \forall\, v \in V,$$

where $a_0(\cdot,\cdot)$ denotes the case $Z \equiv 0$, same as bilinear form $a(\cdot,\cdot)$ in (4).

Coercivity (16) of the bilinear form $a_0(\cdot,\cdot)$ shows that $\lambda_0 > 0$.

Moreover, if $Z(\mathbf{x}) > -\lambda_0$ for all $\mathbf{x} \in \Omega$, then the problem (49) is well posed since it is still coercive.

Let $\epsilon > 0$. Consider the problem

$$-\epsilon \Delta u_\epsilon + u_\epsilon = f \text{ in } \Omega,$$

together with boundary conditions $u = 0$ on $\partial\Omega$, where f is held fixed independent of ϵ.

This is known as a **singular perturbation** problem.

Under certain conditions, we expect $u_\epsilon \to f$ as $\epsilon \to 0$, since this is what we get if the term $\epsilon \Delta u_\epsilon$ goes to zero as $\epsilon \to 0$.

But this can only be correct if $f = 0$ on $\partial\Omega$.

Localized behavior

But in many cases, the data f does not satisfy the constraint $f = 0$ on $\partial\Omega$, and in that case something has to be compromised.

In the typical situation, $u_\epsilon \to f$ as $\epsilon \to 0$ everywhere except in a small **boundary layer** near $\partial\Omega$.

To gain intuition, we consider an example.

Localized behavior

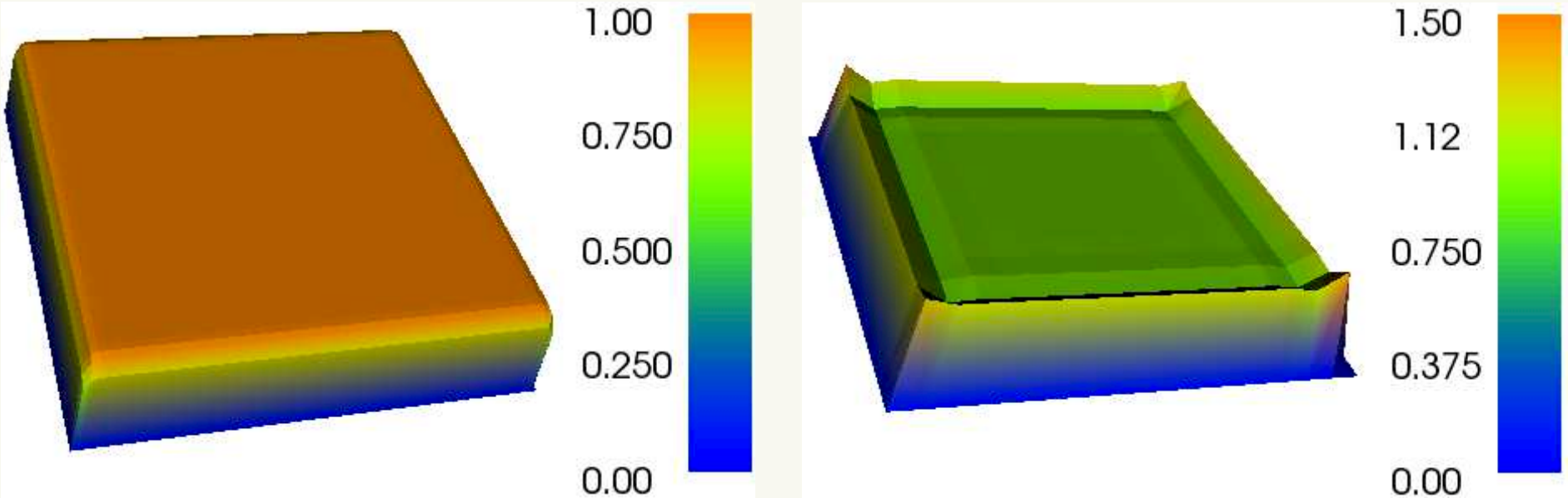

Figure 13: Boundary layer problem with $\epsilon = 0.0001$ and $f \equiv 1$ approximated with piecewise linears: (left) 64×64 mesh and (right) 16×16 mesh.

Computational data

degree	mesh number	L^2 difference	time
1	256	6.86e-02	1.11
1	512	5.34e-02	5.1
1	1024	4.72e-02	29
2	512	4.54e-02	23
4	256	4.48e-02	18
8	128	4.47e-02	25
8	8	7.74e-02	23

Table 6: Boundary layer problem with $\epsilon = 10^{-6}$. Degree refers to the polynomial degree, mesh number indicates the number of edges along each boundary side, L^2 difference is $\|u - f\|_{L^2([0,1]^2)}$, and time is in seconds.

Boundary layer example

degree	mesh number	L^2 difference	ϵ
1	256	1.43e-01	1.00e-04
1	512	1.42e-01	1.00e-04
1	256	8.64e-02	1.00e-05
1	512	8.14e-02	1.00e-05
1	1024	8.00e-02	1.00e-05
1	1024	4.72e-02	1.00e-06

Table 7: Boundary layer problem with various values of ϵ. Degree refers to the polynomial degree, mesh number indicates the number of edges along each boundary side, L^2 difference is $\|u - f\|_{L^2([0,1]^2)}$.

Let $\epsilon > 0$. Consider the problem

$$-\epsilon \Delta u_\epsilon + u_\epsilon = f \text{ in } \Omega = [0,1]^2,$$

together with boundary conditions $u = 0$ on $\partial\Omega$, where $f \equiv 1$ is held fixed independent of ϵ.

In this case, f does not satisfy the boundary conditions.

The solution is depicted in Figure 13.

On the left side of Figure 13, the mesh is fine enough to resolve the boundary layer, but on the right side of Figure 13, we see a numerical artifact (an over-shoot).

In Table 7, we see evidence that $u_\epsilon \to f$ in $L^2(\Omega)$.

Unbounded potentials

For certain unbounded potentials, it is still possible to show that (49) is well posed.

For example, if Z is either the Coulombic or graviational potential $Z(\mathbf{x}) = -|\mathbf{x}|^{-1}$, then the eigenvalue problem

$$a_Z(u_\lambda, v) = \lambda \int_\Omega u_\lambda(\mathbf{x}) v(\mathbf{x})\, d\mathbf{x} \quad \forall\, v \in V,$$

is well posed, even in the case $\Omega = \mathbb{R}^3$.

In this case, eigensolutions correspond to the wave functions of the hydrogen atom [7].

Exercise: explore this problem.

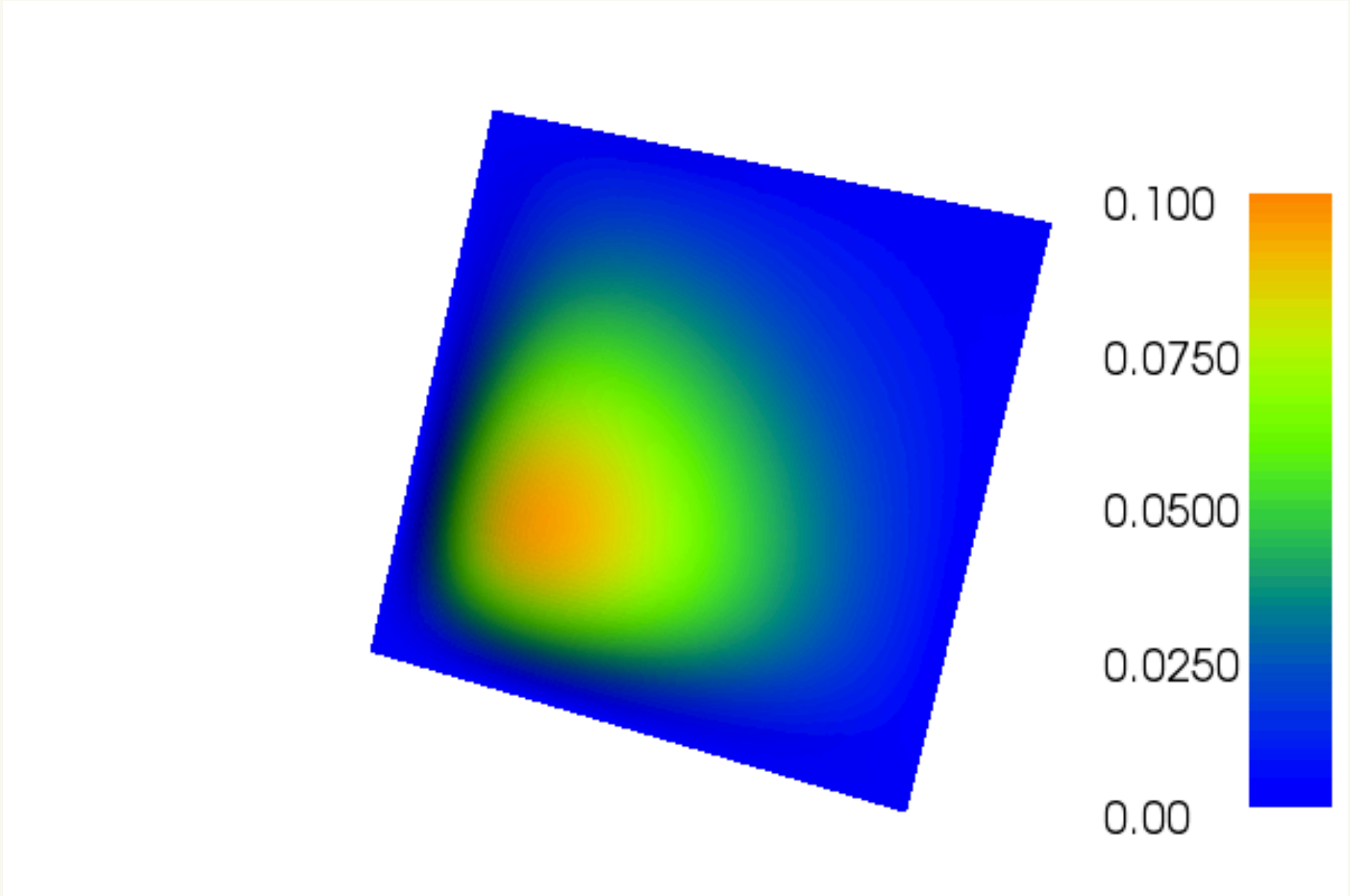

Figure 14: Asymptotic wavefunction perturbation computed with quartics on a mesh of size 100, with $L = 7$.

van der Waals interaction energy between two hydrogen atoms, separated by a distance R, is asymptotically of the form $-C_6 R^{-6}$ where the constant C_6 can be computed [3] by solving a two-dimensional PDE.

Let $\Omega = [0, \infty] \times [0, \infty]$ and consider the PDE

$$\begin{aligned} -\frac{1}{2}\Delta u(r_1, r_2) + \left(\kappa(r_1) + \kappa(r_2)\right) u(r_1, r_2) \\ = -\frac{1}{\pi}(r_1 r_2)^2 e^{-r_1 - r_2} \text{ in } \Omega, \end{aligned} \tag{51}$$

where the function κ is defined by $\kappa(r) = r^{-2} - r^{-1} + \frac{1}{2}$.

The minimum of κ occurs at $r = 2$, and we have $\kappa(r) \geq \frac{1}{4}$.

The problem (51) is well posed in $H_0^1(\Omega)$, i.e., given Dirichlet conditions on the boundary of the quarter-plane Ω.

The variational form for (51) is

$$\begin{aligned} a_\kappa(u,v) = &\int_\Omega \tfrac{1}{2}\nabla u(r_1,r_2)\cdot\nabla v(r_1,r_2)\,dr_1dr_2 \\ &+\int_\Omega \big(\kappa(r_1)+\kappa(r_2)\big)u(r_1,r_2)\,v(r_1,r_2)\,dr_1dr_2, \end{aligned} \tag{52}$$

defined for all $u, v \in H_0^1(\Omega)$.

The form (52) is coercive on $H_0^1(\Omega)$, since $\kappa(r_1) + \kappa(r_2) \geq \frac{1}{2}$. In particular,

$$a_\kappa(v, v) \geq \frac{1}{2} \int_\Omega |\nabla v(r_1, r_2)|^2 + v(r_1, r_2)^2 \, dr_1 dr_2,$$

for all $v \in H_0^1(\Omega)$.

The form $a_\kappa(\cdot, \cdot)$ is continuous on $H_0^1(\Omega)$ because of the Hardy inequality

$$\int_0^\infty \big(u(r)/r\big)^2 \, dr \leq 4 \int_0^\infty \big(u'(r)\big)^2 \, dr$$

for $u \in H_0^1(0, \infty)$.

van der Waals form continuity

Note that it would not be continuous on all of $H^1(0,\infty)$:

without the Dirichlet boundary condition, the form would be infinite for some functions in $H^1(0,\infty)$.

Here is an example of a variational form where

- coercivity is easy to demonstrate
- but continuity is delicate.

To be able to render this problem computationally feasible, we replace Ω by a square Ω_L of side L in length; $\Omega_L = [0, L] \times [0, L]$. Define $U(r_1, r_2) = u(Lr_1, Lr_2)$. Then $\Delta U(r_1, r_2) = L^2 \Delta u(Lr_1, Lr_2)$. Thus

$$
\begin{aligned}
-\frac{1}{2} L^{-2} \Delta U(r_1, r_2) &= -\frac{1}{2} \Delta u(Lr_1, Lr_2) \\
&= -\left(\kappa(Lr_1) + \kappa(Lr_2)\right) u(Lr_1, Lr_2) - \frac{L^4}{\pi} (r_1 r_2)^2 e^{-Lr_1 - Lr_2} \\
&= -\left(\hat{\kappa}_L(r_1) + \hat{\kappa}_L(r_2)\right) U(r_1, r_2) - \frac{L^4}{\pi} (r_1 r_2)^2 e^{-Lr_1 - Lr_2},
\end{aligned}
$$

where $\hat{\kappa}_L(r) = L^{-2} r^{-2} - L^{-1} r^{-1} + \frac{1}{2}$.

Therefore U satisfies

$$-\tfrac{1}{2}L^{-2}\Delta U(r_1,r_2)+(\hat{\kappa}_L(r_1)+\hat{\kappa}_L(r_2))\,U(r_1,r_2)=-\frac{L^4}{\pi}(r_1r_2)^2e^{-Lr_1-Lr_2},$$

which we can pose with homogeneous Dirichlet boundary conditions ($u=0$) on $\Omega_1=[0,1]\times[0,1]$.

Multiplying by $2L^2$, we obtain the equation

$$\begin{aligned}-\Delta U(r_1,r_2)+(\kappa_L(r_1)+\kappa_L(r_2))\,U(r_1,r_2)&=-\frac{2L^6}{\pi}(r_1r_2)^2e^{-Lr_1-Lr_2}\\&=f(r_1,r_2),\end{aligned}\tag{53}$$

where $\kappa_L(r)=2r^{-2}-2Lr^{-1}+L^2$.

Thus we introduce the variational form

$$a_L(u,v) = \int_{[0,1]^2} \nabla u(r_1,r_2)\cdot\nabla v(r_1,r_2) + \big(\kappa_L(r_1)+\kappa_L(r_2)\big)u(r_1,r_2)\,v(r_1,r_2)\,dr_1dr_2 \tag{54}$$

Variational problem: find $u_L \in V = H_0^1([0,1]^2)$ such that

$$a_L(u_L,v) = \int_{[0,1]^2} f(r_1,r_2)\,v(r_1,r_2)\,dr_1dr_2$$

for all $v \in V$.

The solution is shown in Figure 14 with $L = 7$ computed on a mesh of size 100 with quartic Lagrange piecewise polynomials.

The main quantity of interest [3, equation (3.25)] is

$$
\begin{aligned}
C_6 &= -\frac{32\pi}{3}\int_0^\infty\int_0^\infty r_1^2 r_2^2 e^{-(r_1+r_2)} u(r_1,r_2)\,dr_1 dr_2 \\
&\approx -\frac{32\pi}{3}\int_0^L\int_0^L r_1^2 r_2^2 e^{-(r_1+r_2)} u(r_1,r_2)\,dr_1 dr_2 \\
&\approx -\frac{32\pi}{3}\int_0^L\int_0^L r_1^2 r_2^2 e^{-(r_1+r_2)} U(r_1/L,r_2/L)\,dr_1 dr_2 \\
&= -\frac{32\pi}{3}\int_0^1\int_0^1 L^4 R_1^2 R_2^2 e^{-(LR_1+LR_2)} U(R_1,R_2)\,L^2\,dR_1 dR_2 \\
&= -\frac{16\pi^2}{3}\frac{2L^6}{\pi}\int_0^1\int_0^1 R_1^2 R_2^2 e^{-(LR_1+LR_2)} U(R_1,R_2)\,dR_1 dR_2 \\
&= \frac{16\pi^2}{3}\int_0^1\int_0^1 f(R_1,R_2)\,U(R_1,R_2)\,dR_1 dR_2,
\end{aligned}
$$

where we made the substitution $r_i = LR_i$, $i = 1, 2$, and f is defined in (53).

degree	quadrature	mesh no.	C_6 error	ϵ	L	time
4	6	100	4.57e-07	1.00e-09	15.0	1.47
4	10	100	4.57e-07	1.00e-09	15.0	1.595
4	8	250	4.56e-07	1.00e-09	15.0	12.5
2	4	600	4.45e-07	1.00e-09	15.0	4.738
2	2	250	-1.22e-07	1.00e-09	15.0	0.786
2	3	255	-2.74e-08	1.00e-09	15.0	0.786
2	3	265	4.23e-08	1.00e-09	15.0	0.837
2	4	240	-1.87e-08	1.00e-09	15.0	0.739

Table 8: Using finite element computation of $C_6 = 6.4990267054$ [3]. The potential was modified as in (55). Computations were done with 4 cores via MPI and a PETSc Krylov solver. Error values were the same for $\epsilon = 10^{-9}$ and $\epsilon = 10^{-12}$.

To avoid singularities in the coefficients, we modified the potential to be

$$\kappa_L^\epsilon(r) = 2(\epsilon + r)^{-2} - 2L(\epsilon + r)^{-1} + L^2. \tag{55}$$

Computational results are shown in Table 8. The results were insensitive to ϵ for $\epsilon \leq 10^{-9}$.
The singularity $(r_i)^{-2}$ is difficult to deal with. But we can integrate by parts to soften its effect, as follows:

$$\begin{aligned}\int_\Omega (r_i)^{-2} u(r_1, r_2)\, v(r_1, r_2)\, dr_1 dr_2 &= -\int_\Omega \Big(\frac{\partial}{\partial r_i}(r_i)^{-1}\Big) u(r_1, r_2)\, v(r_1, r_2)\, dr_1 dr_2 \\ &= \int_\Omega (r_i)^{-1} \frac{\partial}{\partial r_i}\big(u(r_1, r_2)\, v(r_1, r_2)\big)\, dr_1 dr_2,\end{aligned} \tag{56}$$

where for simplicity we define $\Omega = [0, 1]^2$ here and for the remainder of this subsection.

Another formulation

We have assumed that $u, v \in V = H_0^1(\Omega)$ in (56). Thus

$$\int_\Omega \big((r_1)^{-2} + (r_2)^{-2}\big) u(r_1, r_2)\, v(r_1, r_2)\, dr_1 dr_2$$
$$= \int_\Omega \big((r_1)^{-1}, (r_2)^{-1}\big) \cdot \nabla\big(u(r_1, r_2)\, v(r_1, r_2)\big)\, dr_1 dr_2$$
$$= \int_\Omega \big((r_1)^{-1}, (r_2)^{-1}\big) \cdot \Big(\big(\nabla u(r_1, r_2)\big)\, v(r_1, r_2) + \big(\nabla v(r_1, r_2)\big)\, u(r_1, r_2)\Big)\, dr_1 dr_2$$

Thus we introduce a new variational form (cf. (54))

$$\hat{a}_L^\epsilon(u, v) = \int_\Omega \nabla u(r_1, r_2) \cdot \nabla v(r_1, r_2) + \big(\hat{\kappa}_L^\epsilon(r_1) + \hat{\kappa}_L^\epsilon(r_2)\big) u(r_1, r_2)\, v(r_1, r_2)\, dr_1 dr_2$$
$$+ 2 \int_\Omega \widehat{\boldsymbol{\beta}}(r_1, r_2) \cdot \big(\big(\nabla u(r_1, r_2)\big)\, v(r_1, r_2) + u(r_1, r_2)\big(\nabla v(r_1, r_2)\big)\big)\, dr_1 dr_2$$

where

$$\widehat{\boldsymbol{\beta}}(r_1, r_2) = \big((r_1 + \epsilon)^{-1}, (r_2 + \epsilon)^{-1}\big), \qquad \hat{\kappa}_L^\epsilon(r) = -2L(r + \epsilon)^{-1} + 2L^2.$$

Laguerre Galerkin approximation

Instead of using finite elements, we use Laguerre functions:

$$\sigma_{n,\alpha}(r) = e^{-\alpha r} r^n, \quad n = 1, 2, \ldots.$$

Tensor products of these functions for $\alpha = 1$ are used to approximate the solution on the infinite domain Ω.

To shorten notation, let $\sigma_n = \sigma_{n,1}$.
Integrals can be computed exactly. Thus

$$\int_0^\infty \sigma_n' \sigma_m' \, dr = (m+n-2)! \left((m+n) - (m-n)^2 \right) / 2^{m+n+1}$$

$$\int_0^\infty \sigma_n \sigma_m r^{-i} \, dr = (m+n-i)! / 2^{m+n-i+1}.$$

Define a one-dimensional variational form

$$\hat{a}(u,v) = \int_0^\infty \tfrac{1}{2}u'v' + \kappa(r)uv\,dr. \tag{57}$$

Thus

$$\hat{a}(\sigma_n,\sigma_m) = (m+n-2)!\big((m+n) - (m-n)^2 + 8 - 4(m+n-1) - \lambda_0(m+n)(m+n-1)\big)/2^{m+n+2}.$$

Also need the corresponding "mass" matrix

$$\mu(\sigma_n,\sigma_m) = \int_0^\infty \sigma_n\sigma_m\,dr = (m+n)!/2^{m+n+1}. \tag{58}$$

Now condsider approximation by tensor products

$$v(r_1, r_2) = \sum_{i=1}^{k} \sum_{j=1}^{k} c_{ij} \sigma_i(r_1) \sigma_j(r_2). \tag{59}$$

We seek solutions u of the form (59) to

$$a_\kappa(u, v) = (f, v) \tag{60}$$

for all v of the form (59), where

$$(f, v) = \int_0^\infty \int_0^\infty f(r_1, r_2) v(r_1, r_2)\, dr_1 dr_2. \tag{61}$$

$$f(r_1, r_2) = -\sigma_2(r_1)\sigma_2(r_2). \tag{62}$$

Typical matrix element corresponding to (60):

$$\begin{aligned} A_{(i,j),(m,n)} &= a(\sigma_i(r_1)\sigma_j(r_2), \sigma_m(r_1)\sigma_n(r_2)) \\ &= \hat{a}(\sigma_i, \sigma_m)\mu(\sigma_j, \sigma_n) + \hat{a}(\sigma_j, \sigma_n)\mu(\sigma_i, \sigma_m), \end{aligned} \tag{63}$$

where μ is the mass matrix defined in (58).

When f takes the form (62), the right-hand side in the corresponding linear equation is

$$-\mu(\sigma_2, \sigma_m)\mu(\sigma_2, \sigma_n) = -(m+2)!(n+2)!/2^{m+n+6}, \tag{64}$$

where μ is defined and evaluated in (58).

The quantity of interest C_6 computed as indicated in Table 9.

k	C_6 values	k	C_6 values	k	C_6 values
		6	6.499025	11	6.49902670534
2	6.17	7	6.4990266	12	6.49902670539
3	6.486	8	6.49902669	13	6.499026705401
4	6.4985	9	6.499026703	14	6.499026705404
5	6.49900	10	6.4990267051	15	6.499026705403

Table 9: Convergence of C_6 values as a function of the degree k of polynomials used in the Laguerre function approximation.

Computational details

Using the basis functions σ_n yields matrices with extreme scales.

To compensate, we used diagonal scaling for the linear system.

$Au = f$ was modified to $DADy = Df$ where $u = Dy$.

The diagonal matrix D was chosen to be, in `octave` notation, `D=inv(diag(sqrt(diag(A))))`.

With this scaling, round-off errors only appeared beyond the twelfth digits using sixteen digit computation in `octave`, at least for $k \leq 15$.

References

[1] Wolfgang Bangerth and Rolf Rannacher. *Adaptive Finite Element Methods for Differential Equations*. Birkhäuser, 2013.

[2] Susanne C. Brenner and L. Ridgway Scott. *The Mathematical Theory of Finite Element Methods*. Springer-Verlag, third edition, 2008.

[3] Eric Cancès and L. Ridgway Scott. van der Waals interactions between two hydrogen atoms: The Slater-Kirkwood method revisited. *accepted by SIMA*, TBD, 2017.

[4] Martin Costabel and Monique Dauge. Singularities of electromagnetic fields in polyhedral domains. *Archive for Rational Mechanics and Analysis*, 151(3):221–276, 2000.

[5] Martin Costabel, Monique Dauge, and Christoph Schwab. Exponential convergence of hp-FEM for Maxwell equations with weighted regularization in polygonal domains. *Mathematical Models and Methods in Applied Sciences*, 15(04):575–622, 2005.

[6] Charles L. Epstein and Michael O'Neil. Smoothed corners and scattered waves. *arXiv preprint arXiv:1506.08449*, 2015.

[7] Linus Pauling and E. Bright Wilson. *Introduction to Quantum Mechanics with Applications to Chemistry*. Dover, 1985.

[8] Dominik Schötzau, Christoph Schwab, and Rolf Stenberg. Mixed hp-FEM on anisotropic meshes II: Hanging nodes and tensor products of boundary layer meshes. *Numerische Mathematik*, 83(4):667–697, 1999.

[9] Pavel Šolín, Jakub Červenỳ, and Ivo Doležel. Arbitrary-level hanging nodes and automatic adaptivity in the hp-FEM. *Mathematics and Computers in Simulation*, 77(1):117–132, 2008.

[10] M. N. Vu, S. Geniaut, P. Massin, and J. J. Marigo. Numerical investigation on corner singularities in cracked plates using the G-theta method with an adapted θ field. *Theoretical and Applied Fracture Mechanics*, 77:59 – 68, 2015.